ALMA MATER STUDIORUM

UNIVERSITÀ DI BOLOGNA

School of Engineering and Architecture Department of Electrical, Electronics and Information Engineering “Guglielmo Marconi”

MASTER DEGREE IN ELECTRICAL ENERGY ENGINEERING

THESIS TITLE

Description of Methods and Techniques for Fault Location in Distribution Networks by using PMU

Author:

Syed Muhammad Wahaj Ajmal

Matricola: 0000835827

Supervisor:

Prof. Lorenzo Peretto

ACADEMIC YEAR 2020/21

Abstract:

Whenever a fault occurs in a distribution network or a power grid, accurately and timely locating the fault is of great importance in order to reduce fault losses. With the rapid development of synchronous phasor measurement technology, the high-precision big data brought by synchronous phasor measurement provides ample opportunities for on-line distribution network fault diagnosis. This thesis focuses on the different studies and researches that have been made on the techniques and methods being used currently in Distribution Networks for fault location using PMU. There are several different approaches and studies that this paper will be describing in order to better comprehend these methodologies and see the benefits of these different techniques so that they can be a guide for further research studies in regards to fault location in distribution networks.

Introduction:

1. Distribution Networks:

Electric power distribution is the final stage in the delivery of electric power; it carries electricity from the transmission system to individual consumers. Distribution substations connect to the transmission system and lower the transmission voltage to medium voltage ranging between 2 kV and 35 kV with the use of transformers[1]. Primary distribution lines carry this medium voltage power to distribution transformers located near the customer's premises. Distribution transformers again lower the voltage to the utilization voltage used by lighting, industrial equipment and household appliances. Often several customers are supplied from one transformer through secondary distribution lines. Commercial and residential customers are connected to the secondary distribution lines through service drops. Customers demanding a much larger amount of power may be connected directly to the primary distribution level or the sub transmission level[2].

The transition from transmission to distribution happens in a power substation, which has the following functions[2]:

- Circuit breakers and switches enable the substation to be disconnected from the transmission grid or for distribution lines to be disconnected.
- Transformers step down transmission voltages, 35 kV or more, down to primary distribution voltages. These are medium voltage circuits, usually 600–35000 V[1].
- From the transformer, power goes to the bus bar that can split the distribution power off in multiple directions. The bus distributes power to distribution lines, which fan out to customers.

Urban distribution is mainly underground, sometimes in common utility ducts. Rural distribution is mostly above ground with utility poles, and suburban distribution is a mix [1]. Closer to the customer, a distribution transformer steps the primary distribution power down to a low-voltage secondary circuit, usually 120/240 V in the US for residential customers. The power comes to

the customer via a service drop and an electricity meter. The final circuit in an urban system may be less than 15 metres (50 ft), but may be over 91 metres (300 ft) for a rural customer [1].

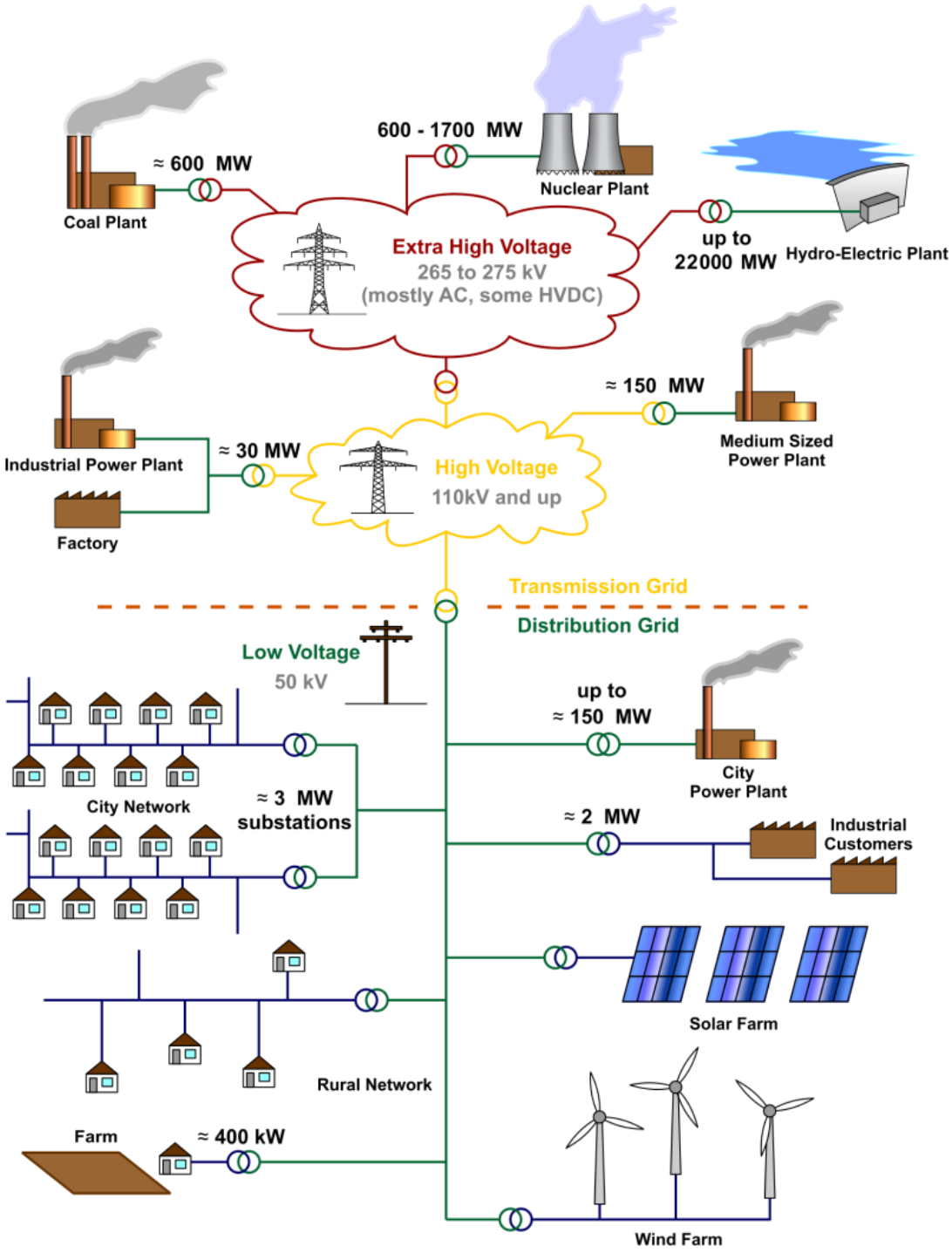

General layout of electricity networks. The voltages and loadings are typical of a European network.

Generation and Transmission:

Electric power begins at a generating station, where the potential difference can be as high as 33,000 volts. AC is usually used. Users of large amounts of DC power such as some railway electrification systems, telephone exchanges and industrial processes such as aluminium smelting use rectifiers to derive DC from the public AC supply, or may have their own generation systems. High-voltage DC can be advantageous for isolating alternating-current systems or controlling the quantity of electricity transmitted. For example, Hydro-Québec has a direct-current line which goes from the James Bay region to Boston[3].

From the generating station it goes to the generating station's switchyard where a step-up transformer increases the voltage to a level suitable for transmission, from 44 kV to 765 kV. Once in the transmission system, electricity from each generating station is combined with electricity produced elsewhere. Electricity is consumed as soon as it is produced. It is transmitted at a very high speed, close to the speed of light.

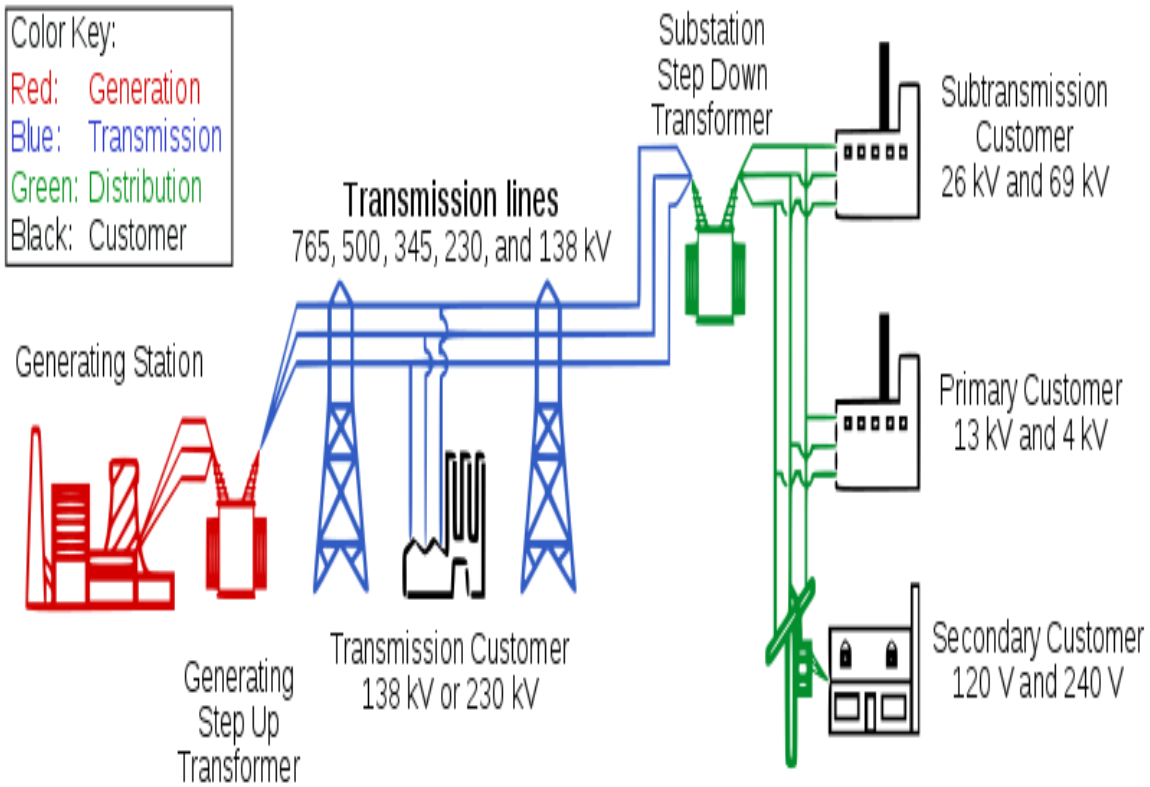

Primary Distribution:

Primary distribution voltages range from 4 kV to 35 kV phase-to-phase (2.4 kV to 20 kV phase-to-neutral)[4] Only large consumers are fed directly from distribution voltages; most utility customers are connected to a transformer, which reduces the distribution voltage to the low voltage "utilization voltage", "supply voltage" or "mains voltage" used by lighting and interior wiring systems.

Network Configurations:

Distribution networks are divided into two types, radial or network[5]. A radial system is arranged like a tree where each customer has one source of supply. A network system has multiple sources of supply operating in parallel. Spot networks are used for concentrated loads. Radial systems are commonly used in rural or suburban areas.

Radial systems usually include emergency connections where the system can be reconfigured in case of problems, such as a fault or planned maintenance. This can be done by opening and closing switches to isolate a certain section from the grid.

Long feeders experience voltage drop (power factor distortion) requiring capacitors or voltage regulators to be installed.

Reconfiguration, by exchanging the functional links between the elements of the system, represents one of the most important measures which can improve the operational performance of a distribution system. The problem of optimization through the reconfiguration of a power distribution system, in terms of its definition, is a historical single objective problem with constraints. Since 1975, when Merlin and Back[6] introduced the idea of distribution system reconfiguration for active power loss reduction, until nowadays, a lot of researchers have proposed diverse methods and algorithms to solve the reconfiguration problem as a single objective problem. Some authors have proposed Pareto optimality based approaches (including active power losses and reliability indices as objectives). For this purpose, different artificial intelligence based methods have been used: microgenetic[7], branch exchange[8], particle swarm optimization[9] and non-dominated sorting genetic algorithm[10].

Rural Services:

Rural electrification systems tend to use higher distribution voltages because of the longer distances covered by distribution lines (see Rural Electrification Administration). 7.2, 12.47, 25, and 34.5 kV distribution is common in the United States; 11 kV and 33 kV are common in the UK, Australia and New Zealand; 11 kV and 22 kV are common in South Africa; 10, 20 and 35 kV are common in China[11]. Other voltages are occasionally used.

Rural services normally try to minimize the number of poles and wires. It uses higher voltages (than urban distribution), which in turn permits use of galvanized steel wire. The strong steel wire allows for less expensive wide pole spacing. In rural areas a pole-mount transformer may serve only one customer. In New Zealand, Australia, Saskatchewan, Canada, and South Africa, Single-wire earth return systems (SWER) are used to electrify remote rural areas.

Three phase service provides power for large agricultural facilities, petroleum pumping facilities, water plants, or other customers that have large loads (Three phase equipment). In North America, overhead distribution systems may be three phase, four wire, with a neutral conductor. Rural distribution system may have long runs of one phase conductor and a neutral[12]. In other countries or in extreme rural areas the neutral wire is connected to the ground to use that as a return (Single-wire earth return). This is called an ungrounded wye system.

Secondary Distribution:

Electricity is delivered at a frequency of either 50 or 60 Hz, depending on the region. It is delivered to domestic customers as single-phase electric power. In some countries as in Europe a three phase supply may be made available for larger properties. Seen with an oscilloscope, the domestic power supply in North America would look like a sine wave, oscillating between −170 volts and 170 volts, giving an effective voltage of 120 volts RMS[13]. Three-phase electric power is more efficient in terms of power delivered per cable used, and is more suited to running large electric motors. Some large European appliances may be powered by three-phase power, such as electric stoves and clothes dryers.

A ground connection is normally provided for the customer's system as well as for the equipment owned by the utility. The purpose of connecting the customer's system to ground is to limit the voltage that may develop if high voltage conductors fall down onto lower-voltage conductors

which are usually mounted lower to the ground, or if a failure occurs within a distribution transformer. Earthing systems can be TT, TN-S, TN-C-S or TN-C.

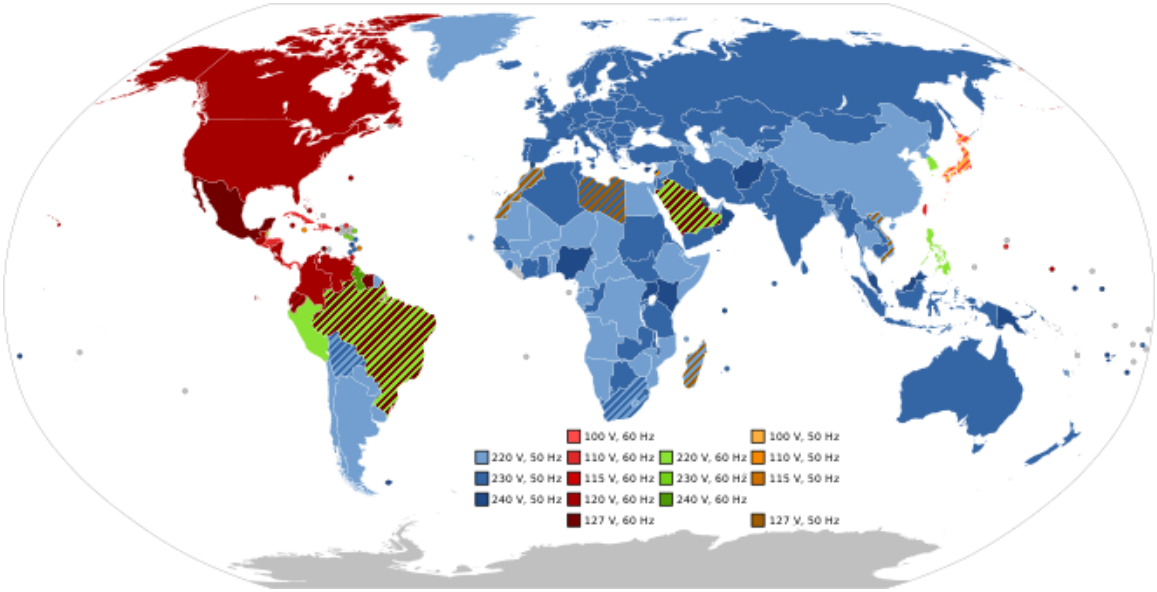

World Map of mains voltage and frequencies

Regional Variations:

220–240 volt systems

Most of the world uses 50 Hz 220 or 230 V single phase, or 400 V 3 phase for residential and light industrial services. In this system, the primary distribution network supplies a few substations per area, and the 230 V / 400 V power from each substation is directly distributed to end users over a region of normally less than 1 km radius. Three live (hot) wires and the neutral are connected to the building for a three phase service. Single-phase distribution, with one live wire and the neutral is used domestically where total loads are light. In Europe, electricity is normally distributed for industry and domestic use by the three-phase, four wire system. This gives a phase-to-phase voltage of 400 volts wye service and a single-phase voltage of 230 volts between any one phase and neutral. In the UK a typical urban or suburban low-voltage substation would normally be rated between 150 kVA and 1 MVA and supply a whole neighborhood of a few hundred houses. Transformers are typically sized on an average load of 1 to 2 kW per household, and the service fuses and cable is sized to allow any one property to draw

a peak load of perhaps ten times this. For industrial customers, 3-phase 690 / 400 volt is also available, or may be generated locally[14]. Large industrial customers have their own transformer(s) with an input from 11 kV to 220 kV.

100–120 volt systems

Most of the Americas use 60 Hz AC, the 120/240 volt split-phase system domestically and three phase for larger installations. North American transformers usually power homes at 240 volts, similar to Europe's 230 volts. It is the split-phase that allows use of 120 volts in the home.

In the electricity sector in Japan, the standard voltage is 100 V, with both 50 and 60 Hz AC frequencies being used. Parts of the country use 50 Hz, while other parts use 60 Hz[15]. This is a relic from the 1890s. Some local providers in Tokyo imported 50 Hz German equipment, while the local power providers in Osaka brought in 60 Hz generators from the United States. The grids grew until eventually the entire country was wired. Today the frequency is 50 Hz in Eastern Japan (including Tokyo, Yokohama, Tohoku, and Hokkaido) and 60 Hz in Western Japan (including Nagoya, Osaka, Kyoto, Hiroshima, Shikoku, and Kyushu) [16].

Most household appliances are made to work on either frequency. The problem of incompatibility came into the public eye when the 2011 Tōhoku earthquake and tsunami knocked out about a third of the east's capacity, and power in the west could not be fully shared with the east, since the country does not have a common frequency[15].

There are four high-voltage direct current (HVDC) converter stations that move power across Japan's AC frequency border. Shin Shinano is a back-to-back HVDC facility in Japan which forms one of four frequency changer stations that link Japan's western and eastern power grids. The other three are at Higashi-Shimizu, Minami-Fukumitsu and Sakuma Dam. Together they can move up to 1.2 GW of power east or west[17].

240 volt systems and 120 volt outlets

Most modern North American homes are wired to receive 240 volts from the transformer, and through the use of split-phase electrical power, can have both 120 volt receptacles and 240 volt

receptacles. The 120 volts is typically used for lighting and most wall outlets. The 240 volt circuits are typically used for appliances requiring high watt heat output such as ovens and heaters. They may also be used to supply an electric car charger.

Modern Distribution Systems:

Traditionally, the distribution systems would only operate as simple distribution lines where the electricity from the transmission networks would be shared among the customers. Today's distribution systems are heavily integrated with renewable energy generations at the distribution level of the power systems by the means of distributed generation resources, such as solar energy and wind energy[18]. As a result, distribution systems are becoming more independent from the transmission networks day-by-day. Balancing the supply-demand relationship at these modern distribution networks (sometimes referred to as micro grids) is extremely challenging, and it requires the use of various technological and operational means to operate. Such tools include battery storage power station, data analytics, optimization tools, etc.

Bibliography:

1. Short, T.A. (2014). *Electric Power Distribution Handbook. Boca Raton, Florida, USA: CRC Press. pp. 1–33. ISBN 978-1-4665-9865-2.*
2. *"How Power Grids Work". HowStuffWorks. April 2000. Retrieved 2016-03-18.*
3. *"Extra-High-Voltage Transmission | 735 kV | Hydro-Québec". hydroquebec.com. Retrieved 2016-03-08.*
4. *Csanyi, Edvard (10 August 2012). "Primary Distribution Voltage Levels". electrical-engineering-portal.com. EEP – Electrical Engineering Portal. Retrieved 9 March 2017*
5. *Abdelhay A. Sallam and Om P. Malik (May 2011). Electric Distribution Systems. IEEE Computer Society Press. p. 21. ISBN 9780470276822.*
6. Merlin, A.; Back, H. Search for a Minimal-Loss Operating Spanning Tree Configuration in an Urban Power Distribution System. In Proceedings of the 1975 Fifth Power Systems Computer Conference (PSCC), Cambridge, UK, 1–5 September 1975; pp. 1–18.

7. Mendoza, J.E.; Lopez, M.E.; Coello, C.A.; Lopez, E.A. Microgenetic multiobjective reconfiguration algorithm considering power losses and reliability indices for medium voltage distribution network. IET Gener. Transm. Distrib. 2009, 3, 825–840.
8. Bernardon, D.P.; Garcia, V.J.; Ferreira, A.S.Q.; Canha, L.N. Multicriteria distribution network reconfiguration considering subtransmission analysis. IEEE Trans. Power Deliv. 2010, 25, 2684–2691.
9. Amanulla, B.; Chakrabarti, S.; Singh, S.N. Reconfiguration of power distribution systems considering reliability and power loss. IEEE Trans. Power Deliv. 2012, 27, 918–926.
10. *Tomoiagă, Bogdan; Chindriş, Mircea; Sumper, Andreas; Sudria-Andreu, Antoni; Villafafila-Robles, Roberto (2013). "Pareto Optimal Reconfiguration of Power Distribution Systems Using a Genetic Algorithm Based on NSGA-II". Energies. **6** (3): 1439–1455. doi:10.3390/en6031439.*
11. *Chan, F. "Electric Power Distribution Systems" (PDF). Electrical Engineering. Retrieved 12 March 2016.*
12. Donald G. Fink, H. Wayne Beatty (ed), *Standard Handbook for Electrical Engineers, Eleventh Edition*, McGraw Hill, 1978, ISBN 0-07-020974-X, page 18-17
13. *"How Power Grids Work". HowStuffWorks. April 2000. Retrieved 2016-03-18.*
14. *"The Bumpy Road to Energy Deregulation". EnPowered. 2016-03-28.*
15. Jump up to:[a] [b] *Gordenker, Alice (2011-07-19). "Japan's incompatible power grids". The Japan Times Online. ISSN 0447-5763. Retrieved 2016-03-12.*
16. *"Electricity in Japan". Japan-Guide.com. Retrieved 2016-03-12.*
17. *"Why Japan's Fragmented Grid Can't Cope". Spectrum.IEEE.org. Retrieved 2016-03-12.*
18. *Fathabad, A. M.; Cheng, J.; Pan, K.; Qiu, F. (November 2020). "Data-Driven Planning for Renewable Distributed Generation Integration". IEEE Transactions on Power Systems. **35** (6): 4357–4368. Bibcode:2020ITPSy..35.4357F. doi:10.1109/TPWRS.2020.3001235. ISSN 1558-0679. S2CID 225734643.*

2. Phasor Measurement Unit (PMU):

A phasor measurement unit (PMU) is a device used to estimate the magnitude and phase angle of an electrical phasor quantity (such as voltage or current) in the electricity grid using a common time source for synchronization. Time synchronization is usually provided by GPS or IEEE 1588 Precision Time Protocol, which allows synchronized real-time measurements of multiple remote points on the grid. PMUs are capable of capturing samples from a waveform in quick succession and reconstructing the phasor quantity, made up of an angle measurement and a magnitude measurement. The resulting measurement is known as a Synchrophasor. These time synchronized measurements are important because if the grid's supply and demand are not perfectly matched, frequency imbalances can cause stress on the grid, which is a potential cause for power outages[1].

PMUs can also be used to measure the frequency in the power grid. A typical commercial PMU can report measurements with very high temporal resolution, up to 120 measurements per second. This helps engineers in analyzing dynamic events in the grid which is not possible with traditional SCADA measurements that generate one measurement every 2 or 4 seconds. Therefore, PMUs equip utilities with enhanced monitoring and control capabilities and are considered to be one of the most important measuring devices in the future of power systems[2]. A PMU can be a dedicated device, or the PMU function can be incorporated into a protective relay or other device[3].

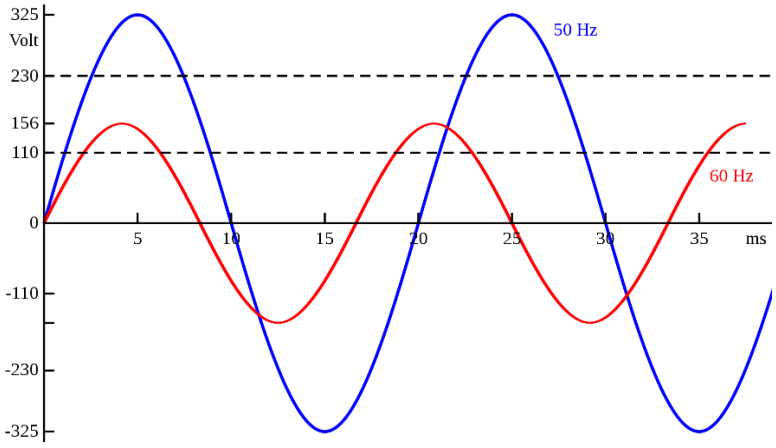

Using a PMU, it is simple to detect abnormal waveform shapes. A waveform shape described mathematically is called a phasor.

Operation:

A PMU can measure 50/60 Hz AC waveforms (voltages and currents) typically at a rate of 48 samples per cycle making them effective at detecting fluctuations in voltage or current at less than one cycle. However, when the frequency does not oscillate around or near 50/60 Hz, PMUs are not able to accurately reconstruct these waveforms. Phasor measurements from PMU's are constructed from cosine waves that follow the structure below[3].

$A\cos(\omega t + \theta)$

The A in this function is a scalar value that is most often described as voltage or current magnitude (for PMU measurements). The θ is the phase angle offset from some defined starting position, and the ω is the angular frequency of the wave form (usually 2π50 radians/second or 2π60 radians/second). In most cases PMUs only measure the voltage magnitude and the phase angle, and assume that the angular frequency is a constant. Because this frequency is assumed constant, it is disregarded in the phasor measurement. PMU's measurements are a mathematical fitting problem, where the measurements are being fit to a sinusoidal curve[3]. Thus, when the waveform is non-sinusoidal, the PMU is unable to fit it exactly. The less sinusoidal the waveform is, such as grid behavior during a voltage sag or fault, the worse the phasor representation becomes.

The analog AC waveforms detected by the PMU are digitized by an analog-to-digital converter for each phase. A phase-locked oscillator along with a Global Positioning System (GPS) reference source provides the needed high-speed synchronized sampling with 1 microsecond accuracy. However, PMUs can take in multiple time sources including non-GPS references as long as they are all calibrated and working synchronously. The resultant time-stamped phasors can be transmitted to a local or remote receiver at rates up to 120 samples per second. Being able to see time synchronized measurements over a large area is helpful in examining how the grid operates at large, and determining which parts of the grid are affected by different disturbances.

Historically, only small numbers of PMUs have been used to monitor transmission lines with acceptable errors of around 1%. These were simply coarser devices installed to prevent catastrophic blackouts. Now, with the invention of micro-synchronous phasor technology, many

more of them are desired to be installed on distribution networks where power can be monitored at a very high degree of precision. This high degree of precision creates the ability to drastically improve system visibility and implement smart and preventative control strategies. No longer are PMUs just required at sub-stations, but are required at several places in the network including tap-changing transformers, complex loads, and PV generation buses[4].

While PMUs are generally used on transmission systems, new research is being done on the effectiveness of micro-PMUs for distribution systems. Transmission systems generally have voltage that is at least an order of magnitude higher than distribution systems (between 12kV and 500kV while distribution runs at 12kV and lower). This means that transmission systems can have less precise measurements without compromising the accuracy of the measurement. However, distribution systems need more precision in order to improve accuracy, which is the benefit of uPMUs. uPMUs decrease the error of the phase angle measurements on the line from ±1° to ±0.05°, giving a better representation of the true angle value[5]. The “micro” term in front of the PMU simply means it is a more precise measurement.

Technical Overview:

A phasor is a complex number that represents both the magnitude and phase angle of the sine waves found in electricity. Phasor measurements that occur at the same time over any distance are called "synchrophasors". While it is commonplace for the terms "PMU" and "synchrophasor" to be used interchangeably they actually represent two separate technical meanings. A synchrophasor is the metered value whereas the PMU is the metering device. In typical applications, phasor measurement units are sampled from widely dispersed locations in the power system network and synchronized from the common time source of a Global Positioning System (GPS) radio clock. Synchrophasor technology provides a tool for system operators and planners to measure the state of the electrical system (over many points) and manage power quality.

PMUs measure voltages and currents at principal intersecting locations (critical substations) on a power grid and can output accurately time-stamped voltage and current phasors. Because these phasors are truly synchronized, synchronized comparison of two quantities is possible in real time. These comparisons can be used to assess system conditions-such as; frequency changes,

MW, MVARs, kVolts, etc. The monitored points are preselected through various studies to make extremely accurate phase angle measurements to indicate shifts in system (grid) stability. The phasor data is collected either on-site or at centralized locations using Phasor Data Concentrator technologies. The data is then transmitted to a regional monitoring system which is maintained by the local Independent System Operator (ISO). These ISO's will monitor phasor data from individual PMU's or from as many as 150 PMU's — this monitoring provides an accurate means of establishing controls for power flow from multiple energy generation sources (nuclear, coal, wind, etc.).

The technology has the potential to change the economics of power delivery by allowing increased power flow over existing lines. Synchrophasor data could be used to allow power flow up to a line's dynamic limit instead of to its worst-case limit.[clarification needed] Synchrophasor technology will usher in a new process for establishing centralized and selective controls for the flow of electrical energy over the grid. These controls will affect both large scale (multiple-states) and individual transmission line sections at intersecting substations. Transmission line congestion (over-loading), protection and control will therefore be improved on a multiple region scale (US, Canada, Mexico) through interconnecting ISO's.

Phasor Networks:

A phasor network consists of phasor measurement units (PMUs) dispersed throughout the electricity system, Phasor Data Concentrators (PDC) to collect the information and a Supervisory Control And Data Acquisition (SCADA) system at the central control facility. Such a network is used in Wide Area Measurement Systems (WAMS), the first of which began in 2000 by the Bonneville Power Administration[6]. The complete network requires rapid data transfer within the frequency of sampling of the phasor data. GPS time stamping can provide a theoretical accuracy of synchronization better than 1 microsecond. "Clocks need to be accurate to ± 500 nanoseconds to provide the one microsecond time standard needed by each device performing synchrophasor measurement." [7] For 60 Hz systems, PMUs must deliver between 10 and 30 synchronous reports per second depending on the application. The PDC correlates the data, and controls and monitors the PMUs (from a dozen up to 60) [8]. At the central control facility, the SCADA system presents system wide data on all generators and substations in the system every 2 to 10 seconds.

PMUs often use phone lines to connect to PDCs, which then send data to the SCADA or Wide Area Measurement System (WAMS) server[9]. Additionally, PMUs can use ubiquitous mobile (cellular) networks for data transfer (GPRS, UMTS), which allows potential savings in infrastructure and deployment costs, at the expense of a larger data reporting latency.[10][11] However, the introduced data latency makes such systems more suitable for R&D measurement campaigns and near real-time monitoring, and limits their use in real-time protective systems.

PMUs from multiple vendors can yield inaccurate readings. In one test, readings differed by 47 microseconds – or a difference of 1 degree of 60 Hz- an unacceptable variance. [12] China's solution to the problem was to build all its own PMUs adhering to its own specifications and standards so there would be no multi-vendor source of conflicts, standards, protocols, or performance characteristics. [13]

Installation:

Installation of a typical 10 Phasor PMU is a simple process. A phasor will be either a 3 phase voltage or a 3 phase current. Each phasor will, therefore, require 3 separate electrical connections (one for each phase). Typically an electrical engineer designs the installation and interconnection of a PMU at a substation or at a generation plant. Substation personnel will bolt an equipment rack to the floor of the substation following established seismic mounting requirements. Then the PMU along with a modem and other support equipment will be mounted on the equipment rack. They will also install the Global Positioning Satellite (GPS) antenna on the roof of the substation per manufacturer instructions. Substation personnel will also install "shunts" in all Current transformer (CT) secondary circuits that are to be measured. The PMU will also require communication circuit connection (Modem if using 4-wire connection or Ethernet for network connection).[4]

Applications:

- Power system automation, as in smart grids
- Load shedding and other load control techniques such as demand response mechanisms to manage a power system. (i.e. Directing power where it is needed in real-time)
- Increase the reliability of the power grid by detecting faults early, allowing for isolation of operative system, and the prevention of power outages.
- Increase power quality by precise analysis and automated correction of sources of system degradation.
- Wide area measurement and control through state estimation,[14] in very wide area super grids, regional transmission networks, and local distribution grids.
- Phasor measurement technology and synchronized time stamping can be used for Security improvement through synchronized encryptions like trusted sensing base. Cyber attack recognition by verifying data between the SCADA system and the PMU data.[15]
- Distribution State Estimation and Model Verification. Ability to calculate impedances of loads, distribution lines, verify voltage magnitude and delta angles based on mathematical state models.
- Event Detection and Classification. Events such as various types of faults, tap changes, switching events, circuit protection devices. Machine learning and signal classification methods can be used to develop algorithms to identify these significant events.
- Microgrid applications—islanding or deciding where to detach from the grid, load and generation matching, and resynchronization with the main grid.[16]

Standards:

The IEEE 1344 standard for synchrophasors was completed in 1995, and reaffirmed in 2001. In 2005, it was replaced by IEEE C37.118-2005, which was a complete revision and dealt with issues concerning use of PMUs in electric power systems. The specification describes standards for measurement, the method of quantifying the measurements, testing & certification requirements for verifying accuracy, and data transmission format and protocol for real-time data communication.[9] This standard was not comprehensive- it did not attempt to address all factors that PMUs can detect in power system dynamic activity.[8] A new version of the standard was released in December 2011, which split the IEEE C37.118-2005 standard into two parts: C37.118-1 dealing with the phasor estimation & C37.118-2 the communications protocol. It also introduced two classifications of PMU, M — measurement & P — protection. M class is close in performance requirements to that in the original 2005 standard, primarily for steady state measurement. P class has relaxed some performance requirements and is intended to capture dynamic system behavior. An amendment to C37.118.1 was released in 2014. IEEE C37.118.1a-2014 modified PMU performance requirements that were not considered achievable.[17]

Other standards used with PMU interfacing:

- OPC-DA / OPC-HDA — A Microsoft Windows based interface protocol that is currently being generalized to use XML and run on non-Windows computers.
- IEC 61850 a standard for electrical substation automation
- BPA PDCStream — a variant of IEEE 1344 used by the Bonneville Power Administration (BPA) PDCs and user interface software.[8]
- IEEE/IEC 60255-118-1-2018 — This part of IEC 60255 is for synchronized phasor measurement systems in power systems. It defines a synchronized phasor (synchrophasor), frequency, and rate of change of frequency measurements. It describes time tag and synchronization requirements for measurement of all three of these quantities. It specifies methods for evaluating these measurements and requirements for compliance with the standard under both static and dynamic conditions. It defines a phasor measurement unit (PMU), which can be a stand-alone physical unit or a functional unit within another physical unit.[18]

Bibliography:

1. "New technology can improve electric power system efficiency and reliability - Today in Energy - U.S. Energy Information Administration (EIA)". *www.eia.gov. Retrieved 2019-05-07.*
2. *Yilu Liu; Lamine Mili; Jaime De La Ree; Reynaldo Francisco Nuqui; Reynaldo Francisco Nuqui (2001-07-12). "State Estimation and Voltage Security Monitoring Using Synchronized Phasor Measurement". Research Paper from Work Sponsored by American Electric Power, ABB Power T&D Company, and Tennessee Valley Authority. Virginia Polytechnic Institute and State University. CiteSeerX 10.1.1.2.7959. Simulations and field experiences suggest that PMUs can revolutionize the way power systems are monitored and controlled. However, it is perceived that costs and communication links will affect the number of PMUs to be installed in any power system.*
3. *Kirkham (December 2016). "Pure and applied metrology". IEEE Instrumentation & Measurement Magazine. **19** (6): 19–24. doi:10.1109/mim.2016.7777647. ISSN 1094-6969.*
4. Jump up to:[a] [b] *"Phasor Advanced FAQ". CERTS. Retrieved 6 January 2013.*
5. *von Meier, Alexandra; Culler, David; McEachern, Alex; Arghandeh, Reza (2014). "Micro-synchrophasors for distribution systems". ISGT 2014. pp. 1–5. doi:10.1109/isgt.2014.6816509. ISBN 9781479936533.*
6. *"Gridwise History: How did GridWise start?". Pacific Northwest National Laboratory. 2007-10-30. Archived from the original on 2008-10-27. Retrieved 2008-12-03.*
7. *KEMA, Inc. (November 2006). "Substation Communications: Enabler of Automation / An Assessment of Communications Technologies". UTC — United Telecom Council: 3–54.*
8. *Cai, J.Y.; Zhenyu Huang; Hauer, J.; Martin, K. (2005). "Current Status and Experience of WAMS Implementation in North America" (PDF). 2005 IEEE/PES Transmission & Distribution Conference & Exposition: Asia and Pacific. pp. 1–7. doi:10.1109/TDC.2005.1546889. ISBN 978-0-7803-9114-7.*
9. *Pei Zhang; J. Chen; M. Shao (October 2007). "Phasor Measurement Unit (PMU) Implementation and Applications (DOCID 1015511)". Electric Power Research Institute (EPRI). Archived from the original (pdf) on 2011-07-10. Retrieved 2008-11-27.*
10. *S. Skok; D. Brnobic; V. Kirincic (August 2011). "Croatian Academic Research Wide Area Monitoring System — CARWAMS" (PDF). Institute of Electrical and Electronics Engineers. Archived from the original (PDF) on 2014-04-29. Retrieved 2011-12-23.*
11. *Brnobic, Dalibor (2013-09-10). "WAMSTER Architecture Details". Wamster.*

12. *A.P. Meliopoulos; Vahid Madani; Damir Novosel; George Cokkinides; et al. (October 2007). "Synchrophasor Measurement Accuracy Characterization". North American SynchroPhasor Initiative Performance & Standards Task Team. Consortium for Electric Reliability Technology Solutions. Archived from the original (pdf) on 2011-07-27. Retrieved 2008-11-27.*
13. *Qixun Yang, Board Chairman, Beijing Sifang Automation Co. Ltd., China and .Bi Tianshu, Professor, North China Electric Power University, China. (2001-06-24). "WAMS Implementation in China and the Challenges for Bulk Power System Protection" (PDF). Panel Session: Developments in Power Generation and Transmission INFRASTRUCTURES IN CHINA, IEEE 2007 General Meeting, Tampa, FL, USA, 24–28 June 2007 Electric Power, ABB Power T&D Company, and Tennessee Valley Authority. Institute of Electrical and Electronics Engineers. Retrieved 2008-12-01.*
14. *Yih-Fang Huang; Werner, S.; Jing Huang; Kashyap, N.; Gupta, V. (September 2012). "State Estimation in Electric Power Grids: Meeting New Challenges Presented by the Requirements of the Future Grid". IEEE Signal Processing Magazine. **29** (5): 33, 43. Bibcode:2012ISPM...29...33H. doi:10.1109/MSP.2012.2187037.*
15. *Mazloomzadeh, Ali; Mohammed, Osama; Zonouz, Saman (2013). "TSB: Trusted sensing base for the power grid". SmartGridComm: 2013 IEEE International Conference on Smart Grid Communications. doi:10.1109/SmartGridComm.2013.6688058. ISBN 978-1-4799-1526-2.*
16. *Alexandra von Meier (2014). "Micro-synchrophasors for Distribution Systems". Proceedings of the International Electrical Congress, Chicago. Innovative Smart Grid Technologies Conference.*
17. *"C37.118.1a-2014 - IEEE Standard for Synchrophasor Measurements for Power Systems -- Amendment 1: Modification of Selected Performance Requirements"*
18. 60255-118-1-2018 - IEEE/IEC International Standard - Measuring relays and protection equipment - Part 118-1: Synchrophasor for power systems – Measurements: https://ieeexplore.ieee.org/document/8577045

3. How does the PMU make the grid more reliable?

A Phasor Measurement Unit, also called a PMU or a synchro phasor, is a key tool used on electric systems to improve operators' visibility into what is happening throughout the vast grid network. A PMU is a device that measures a quantity called a phasor. A phasor tells the magnitude and phase angle for the AC voltage or current at a specific location on a power line. This information can also be used to determine frequency and is useful for identifying and analyzing system conditions.

PMUs provide up to 60 measurements per second, which is much more than the typical one measurement every 2 to 4 seconds provided by conventional SCADA systems. PMUs have a big advantage over traditional means of collecting data because all PMU data is time-stamped using Global Positioning System (GPS) data. This means that data collected across a grid is all synchronized by using the same exact method of associating time with data. For this reason, PMUs are sometimes called synchrophasors. The following illustrates information provided by two PMUs on opposite sides of a transmission line:

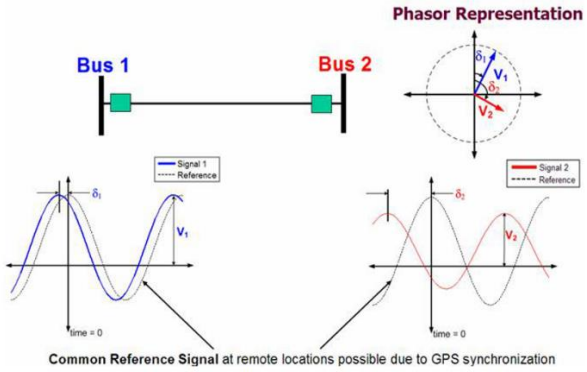

Source: Consortium for Electric Reliability Technology Solutions

PMUs provide a detailed and accurate view of power quality across a wide geographic grid. The data collected tells the system operator if the voltage, current, and frequency is staying within specified tolerances. The capability is used in multiple ways:

- To improve the accuracy of modeling system conditions
- To predict and detect stress and instability on the grid

- To provide information for event analysis after a disturbance has occurred
- To identify inefficiencies
- To predict and manage line congestion

In recent years, tens of thousands of PMUs have been installed in transmission grids throughout the world. In some cases they are also used in distribution grids. Coupled with smart controllers, PMU offer the opportunity to replace typical hands-on adjustments required by SCADA systems with a system that makes decisions and sends control signals autonomously.

Such capabilities promise to allow for more robust and efficient integration of renewables, distributed energy resources (DERs), and microgrids. PMUs are becoming a key tool in making our grid more reliable, resilient, and ultimately cleaner.

4. Methods and Techniques for fault location in Distribution Networks by using PMU:

Augmented State Estimation Method for Fault Location Based on On-line Parameter Identification of PMU Measurement Data

This is the fault location method for augmented state estimation based on on-line parameter identification by using the initial and terminal voltage and current phasor measured by the PMU, the relationship between voltage and current along the positive sequence network and the negative sequence network is inferred. The line fault parameters and information (the fault distance and the voltage phasor from the point of failure are increased in the state quantity and the state estimation is performed with the node state quantity of origin to achieve on-line identification parameters and precise location of the fault. The distribution network model is built in PSCAD. The simulation results verify the accuracy and high precision of the proposed algorithm.

Introduction:

China's medium-voltage power distribution networks generally use small current grounding system which have small ground current when a single-phase ground fault occurs, and short-time grounding will not cause the switch to trip. So it has high power supply reliability. However, operation with fault for a long time will lead to line insulation damage, and even lead to more serious phase-to-phase fault. Therefore, after a fault occurs, accurate and timely fault location is of great significance in reducing fault losses. With the rapid development of synchronous phasor measurement technology, it can accurately describe the real-time behavior characteristics of the distribution network system and can synchronously collect high-precision operating parameters of the distribution network[1-3]. The highprecision big data brought by the synchronous phasor

measurement brings many possibilities to the on-line fault location of the distribution network. At present, the main fault location algorithms can be divided into traveling wave method, impedance method, injection method and artificial intelligence method[4]. Traveling wave method is based on voltage and current traveling wave for line fault location, which is often used for fault location of highvoltage transmission lines. Due to the complicated structure and short line, the application of traveling wave method is limited in distribution system[5-6]. Injection method requires an external signal source, which will have impacts on the operation of the power grid[7]. Artificial intelligence algorithms such as fuzzy algorithm, genetic algorithm and neural network algorithm are mostly in the research stage, and need to train a large number of samples with low reliability[8]. Impedance method can be divided into single-ended method and double-ended method. The single-ended algorithm is affected by the transition resistance, so the distance measurement precision is low. The double-ended method can eliminate the influence of the transition resistance and improve the distance measurement. Therefore, it has a better prospect of application[9].

At present, most location algorithms are based on the known line parameters. Traditional line parameters are calculated by actual measurement under certain conditions, but in the actual operation process, the line parameters will be affected by environmental conditions, which will affects the accuracy of fault location. Therefore, accurate fault parameters are the basis for proper fault analysis before fault location.

In order to solve the error caused by the off-line parameter inaccuracy, an augmented state estimation fault location method based on on-line parameter identification is used. This algorithm is based on the centralized parameter line model considering distributed capacitance. The characteristics of single-phase grounding fault are analyzed, and the fault network is decomposed into positive sequence network and negative sequence network by using symmetric component method. By using the initial and terminal voltage and current phasor measured by PMU, the relationship between voltage and current along the positive sequence network and negative sequence network is deduced. Based on the augmented state estimation theory, the traditional state estimation of branch power measurement and node injection power measurement is transformed into an equivalent current phasor measurement. The measurement equation is constructed. The line parameters and the fault information (the fault distance and the voltage phasor of the fault point) are augmented into the state quantity, and the state estimation is

performed together with the original node state quantity to realize on-line parameter identification and accurate fault location. The radial distribution network model is built in PSCAD. The simulation results verify the correctness and high precision of the proposed algorithm.

AUGMENTED STATE ESTIMATION METHOD FOR FAULT LOCATION:

Augmented State Estimation Method

The traditional state estimation measurement equation for power systems can be described as:

$$z = h(x) + v \qquad (1)$$

Where, z is the m-dimension measurement vector, x is the n-dimension state vector, v is the measurement error vector, h is the non-linear function associated with the measurement z and the state x. The traditional state estimation measurement vector is generally the branch active and reactive power flow, the node active and reactive power, the node voltage amplitude. The state vector to be determined is the node voltage amplitude and phase angle. The measurement equation for the augmented state estimation proposed in this technique is as follows:

$$z = h(x, p) + v \qquad (2)$$

That is, based on the original state estimation, the other parameter vector p expected to be estimated is added to the state vector, assuming that x contains NA state quantities, and p contains NB state quantities, then the augmented state quantity is from the original NA increase to (NA + NB).

Fault location based on double-ended measurement

In this method, the line model adopts a π model considering the distributed capacitance. Figure 1 shows a schematic diagram after a fault occurs. PMU is installed at S and R terminals respectively. The measurement of PMU includes node voltage phasor and branch current phasor.

Therefore, Voltage E_S, E_R and current I_S, I_R at S and R terminals are measurable, d represents the fault distance as a percentage of the total line length. Z is the total line impedance and Y is the total line susceptance.

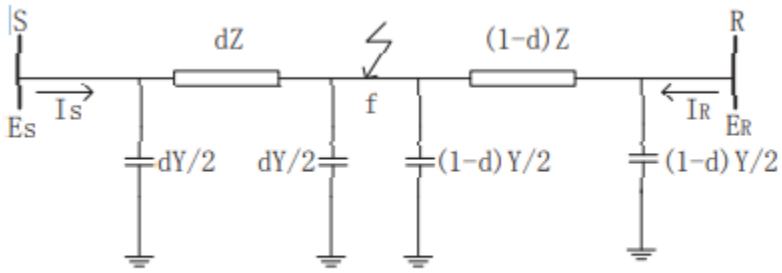

Fig. 1. Sampled faulted line

Taking the most common single-phase-to-ground fault in distribution network as an example, the negative-sequence and zero-sequence network appear in the system after the single-phase-to-ground fault occurs at the f-point of the line. When the distribution network is metallically grounded, the zero-sequence current at the fault point is equal to the sum of the capacitive currents of all non-fault lines to the ground, while the distribution network line is short and the line-to-ground capacitance is small. The zero-sequence current is small, and the zero-sequence current is susceptible to the influence of line distributed capacitance, which makes the fault positioning error larger. Therefore, this method selects the positive sequence network and the negative sequence network after fault for analysis. The positive sequence network and the negative sequence network are respectively shown in Figures 2 and 3.

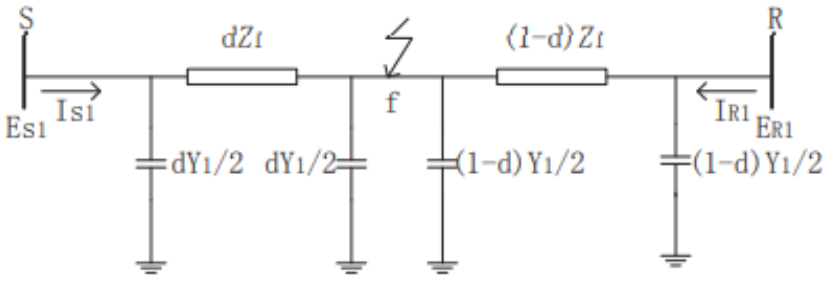

Fig. 2. Fault positive sequence equivalent network

For the circuit shown in Figure 2, the branch voltage and current equations are written to obtain the positive sequence network fault location equation:

$$\begin{cases} \dot{I}_{S1} = \dfrac{(\dot{E}_{S1} - \dot{U}_{f1})}{d \bullet Z_1} + \dfrac{d}{2} \bullet Y_1 \bullet \dot{E}_{S1} \\ \dot{I}_{R1} - \dfrac{(\dot{E}_{R1} - \dot{U}_{f1})}{(1-d) \bullet Z_1} + \dfrac{1-d}{2} \bullet Y_1 \bullet \dot{E}_{R1} \end{cases} \quad (3)$$

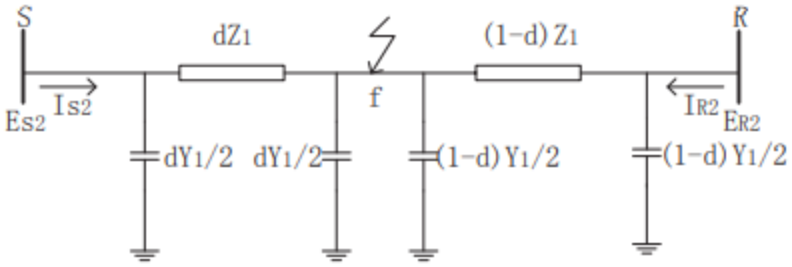

Fig. 3. Fault negative sequence equivalent network

Similarly, the negative sequence network fault location equation is obtained from Figure 3:

$$\begin{cases} \dot{I}_{S2} = \dfrac{(\dot{E}_{S2} - \dot{U}_{f2})}{d \bullet Z_2} + \dfrac{d}{2} \bullet Y_2 \bullet \dot{E}_{S2} \\ \dot{I}_{R2} = \dfrac{(\dot{E}_{R2} - \dot{U}_{f2})}{(1-d) \bullet Z_2} + \dfrac{1-d}{2} \bullet Y_2 \bullet \dot{E}_{R2} \end{cases} \quad (4)$$

In equations (3) and (4), the subscripts 1, 2 represent the parameters of the positive sequence network and the negative sequence network respectively, U_{f1},U_{f2} are the positive sequence voltage and the negative sequence voltage of the fault point.

Proposed location method

In section B, the fault location equations based on double-ended measurement are obtained. Since the positive sequence parameter and the negative sequence parameter of the line are equal, equations (3) and (4) are combined and obtained:

$$\begin{cases} \dot{I}_{S1} = (\dot{E}_{S1} - \dot{U}_{f1}) \bullet \dfrac{1}{d}(g + jb) + \dfrac{d}{2} \bullet Y_1 \bullet \dot{E}_{S1} \\ \dot{I}_{R1} = (\dot{E}_{R1} - \dot{U}_{f1}) \bullet \dfrac{1}{1-d}(g + jb) + \dfrac{1-d}{2} \bullet Y_1 \bullet \dot{E}_{R1} \\ \dot{I}_{S2} = (\dot{E}_{S2} - \dot{U}_{f2}) \bullet \dfrac{1}{d}(g + jb) + \dfrac{d}{2} \bullet Y_1 \bullet \dot{E}_{S2} \\ \dot{I}_{R2} = (\dot{E}_{R2} - \dot{U}_{f2}) \bullet \dfrac{1}{1-d}(g + jb) + \dfrac{1-d}{2} \bullet Y_1 \bullet \dot{E}_{R2} \end{cases} \quad (5)$$

and the unknown state quantity are:

$$x = [d, g, b, y1, \dot{U}_{f1}, \dot{U}_{f2}] \quad (6)$$

Where, 1/Z = g+jb ($Z = Z_1 = Z_2$) is the positive and negative sequence line admittance, Y Y = jy_1 ($Y = Y_1 = Y_2$) is the positive and negative sequence line susceptance. The corresponding measurement equation is obtained by decomposing the imaginary part of the real part:

$$\begin{bmatrix} I_{S1x} \\ I_{S1y} \\ I_{R1x} \\ I_{R1y} \\ I_{S2x} \\ I_{S2y} \\ I_{R2x} \\ I_{R2y} \end{bmatrix} = \begin{bmatrix} h_1(d, g, b, y1, v_{f1}, \theta_{f1}, , v_{f2}, \theta_{f2}) \\ h_2(d, g, b, y1, v_{f1}, \theta_{f1}, , v_{f2}, \theta_{f2}) \\ h_3(d, g, b, y1, v_{f1}, \theta_{f1}, , v_{f2}, \theta_{f2}) \\ h_4(d, g, b, y1, v_{f1}, \theta_{f1}, , v_{f2}, \theta_{f2}) \\ h_5(d, g, b, y1, v_{f1}, \theta_{f1}, , v_{f2}, \theta_{f2}) \\ h_6(d, g, b, y1, v_{f1}, \theta_{f1}, , v_{f2}, \theta_{f2}) \\ h_7(d, g, b, y1, v_{f1}, \theta_{f1}, , v_{f2}, \theta_{f2}) \\ h_8(d, g, b, y1, v_{f1}, \theta_{f1}, , v_{f2}, \theta_{f2}) \end{bmatrix} + \begin{bmatrix} v_1 \\ v_2 \\ v_3 \\ v_4 \\ v_5 \\ v_6 \\ v_7 \\ v_8 \end{bmatrix} \quad (7)$$

Therefore, the new state vector x^{aug} and the new measurement z^{aug} that augmented can be defined as:

$$x^{aug} = [d, g, b, y1, v_{f1}, \theta_{f1}, v_{f2}, \theta_{f2}] \quad (8)$$

$$z^{aug} = [I_{S1x}, I_{S1y}, I_{R1x}, I_{R1y}, I_{S2x}, I_{S2y}, I_{R2x}, I_{R2y}] \quad (9)$$

Now adding the new augmentation measurement equation to the original state estimation measurement equation and get the augmented state estimation method for fault location based on on-line parameter identification. Then using weighted least squares algorithm to solve it. Based on the augmented measurement equation, the optimization goal of the weighted least squares method is:

$$J(x,p)=(z-h(x,p))^{T}W(z-h(x,p)) \qquad (10)$$

Where, W is the weight coefficient matrix. Similar to solving the state estimation based on weighted least squares, the iterative formula for solving (10) is:

$$H_a^{\ T}WH_a\Delta x=H_a^{\ T}W[z-h(x)] \qquad (11)$$

$$\Delta x=[H_a^{\ T}WH_a]^{-1}H_a^{\ T}W[z-h(x)] \qquad (12)$$

where H_a is augmented Jacobian matrix.

$$H_a(x)=\begin{bmatrix} \frac{\partial H_1}{\partial x_1} & \frac{\partial H_2}{\partial x_2} & \cdots & \\ \frac{\partial H_2}{\partial x_1} & \frac{\partial H_2}{\partial x_2} & \cdots & [0] \\ \vdots & \vdots & \ddots & \\ \frac{\partial h_1}{\partial x_1} & \frac{\partial h_1}{\partial x_2} & \cdots & \\ \frac{\partial h_2}{\partial x_1} & \frac{\partial h_2}{\partial x_2} & \cdots & H^{aug} \\ \vdots & & \ddots & \end{bmatrix} \qquad (13)$$

where, dH_m/dx_n is the Jacobian matrix in the original state estimation. H^{aug} is a 8*8 matrix, It includes derivation of new measurement vector z^{aug} with respect to new state vector x^{aug}. The H^{aug} will take the following form:

$$H^{aug}=\begin{bmatrix} \frac{\partial h_1}{\partial d} & \frac{\partial h_1}{\partial g} & \frac{\partial h_1}{\partial b} & \frac{\partial h_1}{\partial y1} & \frac{\partial h_1}{\partial v_{f1}} & \frac{\partial h_1}{\partial \theta_{f1}} & \frac{\partial h_1}{\partial v_{f2}} & \frac{\partial h_1}{\partial \theta_{f2}} \\ \vdots & \vdots & \vdots & \vdots & \vdots & \vdots & \vdots & \vdots \\ \frac{\partial h_8}{\partial d} & \frac{\partial h_8}{\partial g} & \frac{\partial h_8}{\partial b} & \frac{\partial h_8}{\partial y1} & \frac{\partial h_8}{\partial v_{f1}} & \frac{\partial h_8}{\partial \theta_{f1}} & \frac{\partial h_8}{\partial v_{f2}} & \frac{\partial h_8}{\partial \theta_{f2}} \end{bmatrix} \quad (14)$$

Now, completed the design of the entire algorithm is achieved, and now simulation and verification is performed.

SIMULATION AND VERIFICATION:

Simulation model

To verify the correctness of the proposed fault location method, a 10 kV radian distribution network is built based on PSCAD as Figure 4. In the simulation system, the positive sequence resistance and zero sequence resistance per unit length are r_1= 0.0341Ω/km and r_0= 0.2862Ω/km respectively. The positive sequence and zero-sequence inductance per unit length are x_1= 0.2859Ω/km and x_0= 0.1421Ω /km respectively, and the positive sequence and zero-sequence susceptance per unit length are y_1=0.4057x10^{-5} Ω/km and y_0= 0.1549 x 10^{-5} Ω/km respectively.

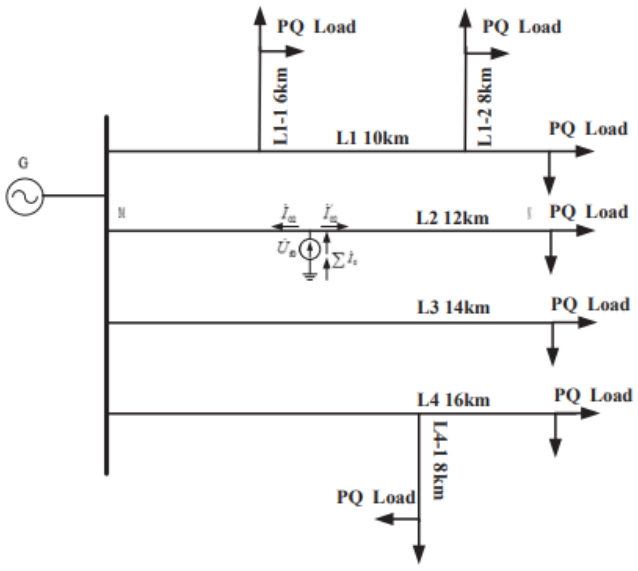

Fig. 4. Radial distribution network model

The fault occurs on L2 line which total length is 12 km. The fault location accuracy is measured by equation (9):

$$E_r = \frac{d \bullet l - D_{real}}{l} \times 100\% \qquad (15)$$

Where D_{real} is the actual fault distance. l is the total length of line, d is the percentage of fault distance in the total line.

Result analysis

In order to verify the correctness of the proposed method, simulating the following situations: under different fault types, under different transition resistances, and when the line parameters change. Then the analysis of location results is given.

Fault location results under different fault types:

Setting distribution network as neutral point non-grounding operation, when fault occurs in L2 line, Fault location results under different fault types are shown in Table 1. According to the location result, it has high precision under different fault types (single-phase to ground, two-phase shorting cut, two-phase to ground). When asymmetric faults occur in the system, negative sequence components will appear in the network, so the proposed algorithm is applicable to asymmetric faults in the network.

TABLE I. SIMULATION RESULT UNDER DIFFERENT FAULT TYPE

Fault type	Fault distance /km	Caculated distance /km	Error/%
AG	3	3.0324	0.2700
	6	6.0435	0.2792
	9	9.1024	0.8533
AB	3	3.0453	0.3775
	6	6.0268	0.2233
	9	9.1109	0.9242
ABG	3	2.9801	-0.1658
	6	6.0188	0.1567
	9	8.8923.	-0.1475

Fault location results under different transition resistance:

Taking the neutral point ungrounded system as an example, the fault location results under different transition resistances are shown in Table 2. It can be seen that the method is based on the principle of double-ended impedance method, and the voltage at the fault point is expressed by the voltage at the initial and the end of the line, eliminated the influence of the transition resistance based on the traditional single-terminal impedance method. Therefore, in this algorithm, the location accuracy is not affected by the change of the transition resistance, and the accuracy and stability of the algorithm are basically not affected by the transition resistance.

TABLE II. SIMULATION RESULT UNDER DIFFERENT TRANSITION RESISTANCE

R_f / Ω	Fault distance /km	Caculated distance /km	Error/%
0	3	3.0324	0.2700
	6	6.0435	0.2792
	9	9.1024	0.8533
10	3	3.0365	0.3042
	6	6.0317	0.2642
	9	9.0813	0.6775
50	3	3.0402	0.3350
	6	6.0478	0.3983
	9	9.0917	0.7642
100	3	3.0416	0.3467
	6	6.0356	0.2967
	9	9.1002	0.8350

Fault location results when the line parameters change:

Set the line parameters to be accurate, the line parameter changes by +5%, and the line parameter changes by -5%. The algorithm is verified under different fault distances. The results are shown in Table 3. It can be seen that when the parameters change, the accuracy of the distance measurement will not be affected. Therefore, the proposed algorithm based on online parameter

estimation, which eliminates the influence of parameter inaccuracy on ranging. Since the proposed method calculates the line parameters and the fault distance at the same time through the augmented state estimation, the error caused by the inaccurate line parameters on the location result can be avoided.

TABLE III. SIMULATION RESULT WHEN THE LINE PARAMETERS CHANGE

Fault distance /km	Line prameter	Caculated distance/km	Error/%
3	accurate	3.0324	0.2700
	change +5%	3.0428	0.3567
	change -5%	3.0389	0.3242
6	accurate	6.0268	0.2233
	change +5%	6.0319	0.2658
	change -5%	5.9743	-0.2142
9	accurate	8.8923.	-0.1475
	change +5%	8.8897	-0.9192
	change -5%	9.0224	0.1867

CONCLUSION:

In this method, the distribution network is taken as the research object, and the more accurate 3 equivalent line model considering the distributed capacitance is adopted. Aiming at the problem that the traditional line parameters have errors in actual operation, which will affect the results of fault location. Line parameter identification is introduced, and augmented state estimation method for fault location based on on-line parameter identification of PMU measurement data is proposed. This algorithm is based on the synchronous data of two terminals collected by PMU. It can estimate the line parameters synchronously on-line in real time, which reduces the error of line parameters inaccurate to fault location results. The simulation results show that the proposed method is not affected by fault type, transition resistance and inaccurate line parameters, and can ensure high location results.

Bibliography:

1. Augmented State Estimation Method for Fault Location Based on On-line Parameter Identification of PMU Measurement Data by Junjuan Li, Xiaojun Wang, Xinyu Ren, Yongjie Zhang, Fang Zhang School of Electrical Engineering Beijing Jiaotong University Beijing 100044 China 17126007@bjtu.edu.cn
2. Roberts C M, Shand C M, Brady K W, et al. Improving distribution network model accuracy using impedance estimation from microsynchrophasor data[C]// IEEE Power and Energy Society General Meeting. IEEE, 2016:1-5.
3. Liao A L, Stewart E M, Kara E C. Micro-synchrophasor data for diagnosis of transmission and distribution level events[C]// Ieee/pes Transmission and Distribution Conference and Exposition. IEEE, 2016:1-5.
4. Von Meier A, Culler D, Mceachern A, et al. Micro-synchrophasors for distribution systems[C]// IEEE Power & Energy Society Innovative Smart Grid Technologies Conference. IEEE, 2014:1-5.
5. Ma Shicong,Gao Houlei,Xu Bingzhen,Xue Yongduan.Overview of Fault Location Technology for Distribution Network[J].Power System Protection and Control,2009,37(11):119-124.
6. Mohammad Farshad,Javad Sadeh. Transmission line fault location using hybrid wavelet-Prony method and relief algorithm[J]. International Journal of Electrical Power and Energy Systems,2014,61.
7. Jing Wang,Xiao Liu,Zhi Yuan Pan. A New Fault Location Method for Distribution Network Based on Traveling Wave Theory[J]. Advanced Materials Research,2015,3701(1070).
8. Yong, C. Wei, L. Jiansheng, elt. "Single phase to earth fault location method in distribution network based on signal injection principle," 2011 4th International Conference on Electric Utility Deregulation and Restructuring and Power Technologies (DRPT), 2011, pp. 204-208.
9. Xu Wen-shang, Wang Wen-wen, Zhang Ni. Research on the Method of Diagnosing Fault and Locating Fault Sources Using Neural Network.IEEE Intelligent Computation Technology and Automation,2008,901-905.
10. Yuan Liao. A Novel Fault Location Method for Radial Distribution Systems[J]. International Journal of Emerging Electric Power Systems,2015,16(3).

Determination of Optimal PMU Placement for Fault-Location Observability

This is a new method to find the minimum number of Phasor Measurement Units (PMU) to determine fault locations on transmission power lines in a power system. Considering the cost of installing the PMUs, it is important to study the scheme of PMU placement at minimal locations in the network in the sense that fault location observability can be achieved throughout the network. In this method, a new algorithm is presented to find an optimization problem, determine the location and the minimum number of PMUs to find the exact location of a fault in power systems. The accuracy of the proposed algorithm is independent of the type of fault and its resistance. The optimization problem is solved using the branch and bond method. 41-bus 230kV Tehran Transmission Regional Electric Network is used as a real case study.

Introduction:

Phasor Measurement Units (PMUs) using synchronization signals from the GPS satellite system have evolved into mature tools and are now being manufactured commercially[1]. In power systems, high voltage transmission and distribution lines are vital links that achieve the essential continuity of service from the generating plants to the end users. Fault location on transmission lines is thus a very well-known and important problem that has been studied for a long time. From views of economics and quality of power feeding, the importance of fault location of transmission lines is increasingly. The more accuracy of fault location has been obtained the easier task for inspection, maintenance, and repair of the line can be achieved. Rapid restoration of service could reduce customer complaints, outage time, loss of revenue, and crew repair expense[2-3]. Several two terminal fault location algorithms based on phasor measurement units (PMUs) techniques have been proposed recently[4-5]. These PMU-based algorithms propose the calculation of fault location using synchronized voltage and current phasors. While they can achieve high accuracy in fault location, they are limited to locate faults in a transmission network in stalled by PMUs on every bus. Considering the installation cost of PMUs, it is important to

investigate the placement scheme of the PMUs at minimal locations on the network in the sense that the fault location observability can be achieved over the entire network[6]. This method presents a new concept of fault location observability and a new fault location scheme for transmission networks based on synchronized PMUs. Considering the high cost of phasor measurement units, minimizing the number of PMUs is very significant. In this method, a new algorithm is introduced to find an optimization problem for determining the place and minimum number of phasor measurement units in order to find accurate place of any fault among power systems. PMUs are placed on the buses by the so called "one bus spaced placement strategy," which means that every two PMUs are spaced by one bus as possible as that the minimal PMUs are achieved. The accuracy of suggested algorithm is independent from the fault types and the fault resistance. The optimization problem may have multiple solutions, in other words a minimum number of PMUs can be spread out over the network in different forms satisfying constraints. The optimization problem is solved by branch and bound[7]. The 41-bus Tehran Transmission Regional Electric Network is used as a real case study.

MINIMAL PMU PLACEMENT:

A PMU placed at a given bus is capable of measuring the voltage phasor of the bus as well as the phasor currents for all lines incident to that bus. Thus, the entire parameters of a bus can be made observable by placing PMUs at strategic buses in the system. The aim of minimal PMU placement strategy is to investigate optimal placement scheme of PMUs to observe the location of faults. Fig 1 illustrates a 7-bus example system. Every general network can be composed of five sub- networks, type-1 to type-5 as shown in Fig 2[6]. In this figure the placement of the PMUs is shown. Each of the five subnetworks is placed with PMUs, which are called "one bus spaced deployment strategy." Indeed, most power transmission networks are composed of these five subnetwork configurations.

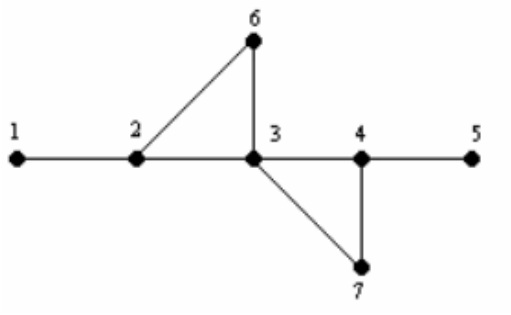

Fig. 1. 7-bus example system.

In the type-2 subnetwork, by using previous described methods, it is easy to determine the location of fault on the line 1-2, because at the both end of this line, PMUs are installed. So the new problem, in this method solved, is determining of fault location on the lines 2-3 and 1-3. It is easy to observe this type of fault location is similar to determine the location of fault on the type-1 subnetwork. Using the similar method, entire subnet- works can be changed to type-1 subnetwork[6]. So determining of fault locations is described only for the type-1 subnetwork.

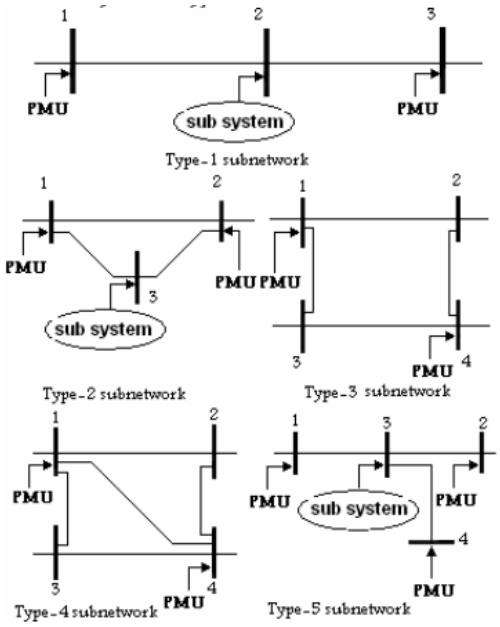

Fig. 2. Five possible subnetworks with one bus spaced method.

Essential measurements for fault location detection algorithm obtained from one bus space installed PMUs. By this method the fault location observability is achieved over the entire network Fig 3 shows a fault on type-1 subnetwork in details.

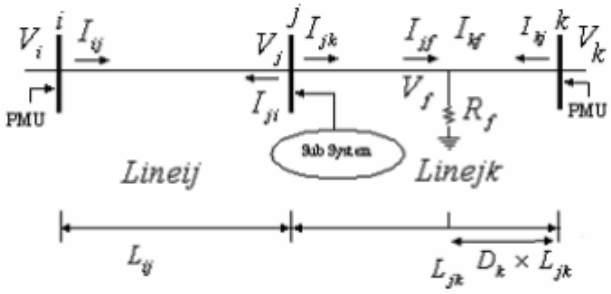

Fig. 3. Type-1 subnetwork with fault.

To clear the details of the method, minimal PMU placement is performed on the 7-bus example system. For fault location observability it is necessary to equip one spaced buses with PMUs. So in Fig 1, one of the buses number 1 or number 2 should be equipped by a PMU. Using the same method one of the buses number 2 or number 6 should be equipped by a PMU. The main purpose of performing this method is to minimize the number of installed PMUs, so for nbus system an optimization problem is used:

$$\min \sum_{i}^{n} x_i \qquad (1)$$

$$s.t. \quad f(x) \geq \hat{1}$$

Where, X is a binary decision variable vector, whose entries are defined as:

$$x_i = \begin{cases} 1 & \text{if a PMU is installed at bus } i \\ 0 & \text{otherwise} \end{cases} \qquad (2)$$

is a vector whose entries are all ones. f (X) is a vector function, whose entries are non-zero if the corresponding bus voltage is solvable using the given measurement set and zero otherwise. The con straints for the 7- bus example system can be formed as:

$$f(x)=\begin{cases} x_1+x_2\geq 1 \\ x_2+x_3\geq 1 \\ x_2+x_6\geq 1 \\ x_3+x_4\geq 1 \\ x_3+x_6\geq 1 \\ x_3+x_7\geq 1 \\ x_4+x_7\geq 1 \\ x_4+x_5\geq 1 \end{cases} \qquad (3)$$

The operator "+" serves as the logical "OR" and the use of 1 in the right hand side of the inequality ensures that at least one of the variables appearing in the sum will be non-zero. For example, consider the third line of constraints as given below:

$$x_2+x_6\geq 1$$

It implies that at least one PMU should be placed at either one of the buses 2 or 6 (or both). Solving this optimization problem by Branch and Bound method, one bus spaced PMU placement is achieved. The results of implementing the proposed method on the 7-bus example system, is shown in Table I:

TABLE I
OPTIMAL PLACEMENT OF PMUS FOR THE 7-BUS EXAMPLE SYSTEM.

Number of PMUs	buses for optimal PMU placement
3	2,3,4

FAULT LOCATION DETECTION:

To determine Dk (p.u.), which is fault location in Fig. 1, phasor measurements of the bus i and bus k are used. The length of the lines in the real case study net work, are in the range of medium length lines, so π line model is used for modeling the lines of the network. Figure 4 shows the details of the Fig. 3 by using the π line model.

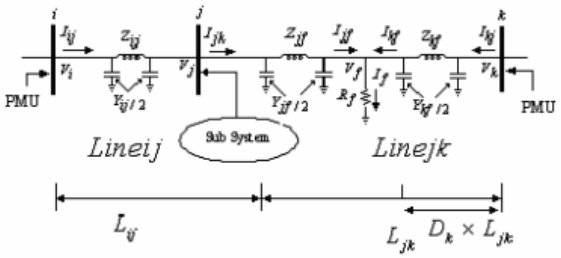

Fig. 4. Development of type-1 subnetwork.

The fault location determination method is intro duced only for three phase faults. By using similar method the location of other fault types can be determined. In Figure 4, by using the voltage phasor of bus i and the parameters of line i-j, the voltage phasor of bus j is determined.

$$V_j = V_i - (I_{ij} - V_i \cdot L_{ij} \cdot Y_{ij} / 2) \cdot L_{ij} \cdot Z_{ij} \qquad (4)$$

In Figure 4 for determining the current phasor Ijk, injected current phasor to bus j is needed. Because there is no PMU installed at bus j, injected current phasor to bus j and so current phasor Ijk can't be calculated. Therefore, there are two unknown variables Ijk and Dk left to be solved. According to the circuit theories and assumption constraints, the two groups of equations for two unknown variables are defined as:

Group-1: Network equations

$$F_1(I_{jk}, D_k, \theta) = 0$$

Group-2: Constraint equations

$$F_2(I_{jk}, D_k, \theta) = 0$$

Where represents the known variables, such as Vi, Vj, Vk, etc. Using the group-1 equations and unknown parameter Dk, voltage and current phasors of the fault is calculated. The Group-2 equations are obtained from the assumption of pure resistance fault impedance. Since the simultaneous equations of Group-1 and Group-2 are nonlinear, a numerical method is needed to find the unknown variables Ijk and Dk. The method of obtaining two groups of equations for three phase faults is introduced as:

$$V_f = V_k - (I_{kj} - V_k \cdot Y_{kf}/2) \cdot Z_{kf} \qquad (5)$$

where:

$$Z_{kf} = Z_{jk} \cdot D_k$$
$$Y_{kf} = Y_{jk} \cdot D_k$$

Which Zjk and Yjk are the impedance (Ω) and shunt admittance (mho) of the line between j and k respectively. Using equation (5), the fault voltage phasor (Vf) can be obtained as a function of unknown parameter Dk.

$$I_{jk} = (V_j - V_f)/Z_{jf} + V_j \cdot Y_{jf}/2 \qquad (6)$$

where:

$$Z_{jf} = (1 - D_k) \cdot Z_{jk}$$
$$Y_{jf} = (1 - D_k) \cdot Y_{jk}$$

Using equation (6), current phasor (Ijk) can be obtained as a function of unknown parameter Dk. Fault current phasor can be achieved from equation (7).

$$I_f = I_{kf} + I_{jf} \qquad (7)$$

where:

$$I_{kf} = (V_k - V_f)/Z_{kf} - V_f \cdot Y_{kf}/2 \qquad (8)$$
$$I_{jf} = (V_j - V_f)/Z_{jf} - V_f \cdot Y_{jf}/2 \qquad (9)$$

Equations (5) and (7) are the group-1 equations. As same as what was explained before, group-2 equations are obtained from the assumption of pure resistance fault impedance to solve the fault location Dk. This consideration makes the angle of fault current and voltage phasor, equal.

$$V_f = \mathrm{Re}\{V_f\} + j\,\mathrm{Im}\{V_f\} \qquad (10)$$
$$I_f = \mathrm{Re}\{I_f\} + j\,\mathrm{Im}\{I_f\} \qquad (11)$$

By assumption of pure resistance fault impedance:

$$Arg\{V_f\} = Arg\{I_f\} \qquad (12)$$

so:

$$\frac{\mathrm{Im}\{I_f\}}{\mathrm{Re}\{I_f\}} = \frac{\mathrm{Im}\{V_f\}}{\mathrm{Re}\{V_f\}}$$

$$\mathrm{Im}\{I_f\} \cdot \mathrm{Re}\{V_f\} = \mathrm{Re}\{I_f\} \cdot \mathrm{Im}\{V_f\} \qquad (13)$$

Considering three phase faults, Eq. (13) is the group 2 equations. Simultaneously solving the proposed fault location equations caused to determine the unknown parameter Dk that is the location of fault on the line between bus j and bus k. Table II shows summary of the two groups of equations for fault location detection:

TABLE II
SUMMARY OF THE TWO GROUPS OF EQUATIONS FOR FAULT LOCATION DETECTION.

Group 1: Network equations (n=0,1,2,)	
$V_{fn} = V_{kn} - (I_{kjn} - V_{kn} \cdot Y_{kfn}/2) \cdot Z_{kfn}$ $I_{jkn} = (V_{jn} - V_{fn}) / Z_{jfn} + V_{jn} \cdot Y_{jfn}/2$ $I_{fn} = (V_{kn} - V_{fn}) / Z_{kfn} - V_{fn} \cdot Y_{kfn}/2$ $+ (V_{jn} - V_{fn}) / Z_{jfn} - V_{fn} \cdot Y_{jfn}/2$	
Group 2: Constraint equations	
a-g fault	$\mathrm{Re}\{I_{f0} + I_{f1} + I_{f2}\} \cdot \mathrm{Im}\{V_{f0} + V_{f1} + V_{f2}\}$ $= \mathrm{Im}\{I_{f0} + I_{f1} + I_{f2}\} \cdot \mathrm{Re}\{V_{f0} + V_{f1} + V_{f2}\}$
b-c-s fault	$\mathrm{Re}\{I_{f1} - I_{f2}\} \cdot \mathrm{Im}\{V_{f1} - V_{f2}\}$ $= \mathrm{Im}\{I_{f1} - I_{f2}\} \cdot \mathrm{Re}\{V_{f1} - V_{f2}\}$
b-c-g fault	$V_{f1} = V_{f2}$
a-b-c-g fault	$\mathrm{Re}\{I_{f1}\} \cdot \mathrm{Im}\{V_{f1}\} = \mathrm{Im}\{I_{f1}\} \cdot \mathrm{Re}\{V_{f1}\}$

Results:

Matlab programming language is used to implement the proposed PMU optimal placement and fault location detection algorithm. This program is tested by applying on 41-bus Tehran Transmission Regional Electric Network (Figure 5). According to what was explained before, in the developed program the proposed algorithm to find optimization constrains is used. The optimization problem is solved by branch and bound method. Table III shows the optimal buses

chose to install the PMUs. Finally the fault location detection algorithm is written. The input data of the program are the π line parameters and measured voltage and current phasors.

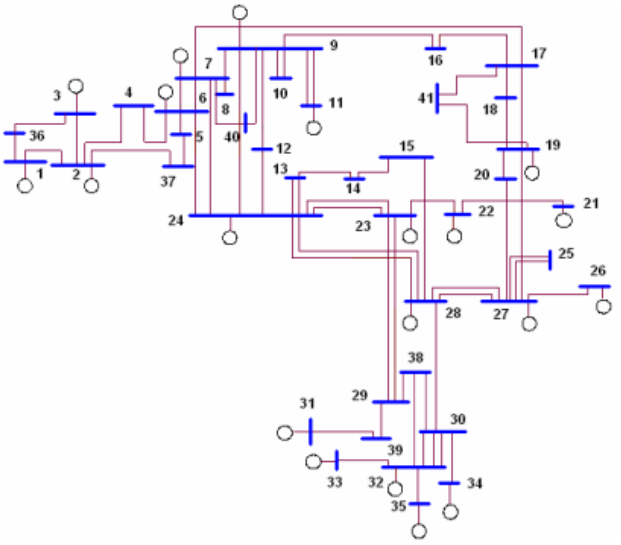

Fig. 5. Single line diagram of the Tehran Transmission Regional Electric Network.

TABLE III
THE OPTIMAL PMU PLACEMENT SCHEME FOR TEHRAN TRANSMISSION REGIONAL ELECTRIC NETWORK.

Total number of PMUs	Number of buses
17	2,5,6,7,9,14,17,19,22,24,27,28,29,30,31,32,36

Conclusion:

A new concept of fault location observability and a new fault location scheme have been presented when using PMUs. The proposed optimization problem has two advantages. First it is economical and second it can be implemented on interconnected networks. The proposed method has been introduced in two steps. First step is to determine the optimal number and place of PMUs among all the network buses. Second step is determining the location of fault by using the installed PMU measurements. The results show the developed method is successful in finding optimal PMU placement and accurate fault location detection. By using branch and bound method, an optimal PMU arrangement has been achieved. As shown in Table III, for fault location detection observability, at least 17 installed PMUs are needed.

Bibliography:

1. Determination of Optimal PMU Placement for Fault-Location Observability by K. Mazlumi, H. Askarian Abyaneh, S. H. H. Sadeghi, and S. S. Geramian
2. Phadke, A.G., "Synchronized phasor measurements in power systems," IEEE Computer Applications in Power, Volume 6, Issue 2, April 1993 Page(s):10 – 15.
3. Damir Novosell, David G. Hart, Eric Udren, and Murari Mohan Saha, "Fault Location Using Digital Relay Data," IEEE Computer Applications in Power, Volume 8, Issue 3, July 1995 Page(s): 45 - 50 July 1995. DRPT2008 6-9 April 2008 Nanjing China.
4. Javad Sadeh, N. Hadjsaid, A. M. Ranjbar, and R. Feuillet, "Accurate Fault Location Algorithm for Series Compensated Transmission Lines," IEEE Transaction on Power Delivery, Volume 15, Issue 3, July 2000 Page(s):1027 – 1033.
5. Chi-Shan Yu, Chih-Wen Liu, Ying-Hong Lin, "A Fault Location Algorithm for Transmission Lines with Tapped Leg-PMU Based Approach," IEEE Power Engineering Society Summer Meeting, Volume 2, 15-19 July 2001 Page(s):915 – 920.
6. Ying-Hong Lin, Chih-Wen Liu, and Ching-Shan Chen, "A New PMUBased Fault Detection/Location Technique for Transmission Lines With Consideration of Arcing Fault Discrimination-Part I: Theory and Algorithms," IEEE Transaction on Power Volume 19, Issue 4, Oct. 2004 Page(s):1587 – 1593.
7. Kai-Ping Lien, Chih-Wen Liu, Chi-Shan Yu, and Joe-Air Jiang, "Transmission Network Fault Location Observability With Minimal PMU Placement," IEEE Transaction on Power Delivery, Volume 21, Issue 3, July 2006 Page(s):1128 – 1136.
8. Bei Xu, A. Abur, "Optimal Placement and Utilization of Phasor Measurements for State Estimation", Power System Computation Conference, August 2005, Liege, Belgium.

Fault Location Method Using Phasor Measurement Units and Short Circuit Analysis for Power Distribution Networks

To improve the problems of existing studies, this method focuses on different approaches such as in order to minimize the number of PMU installations, an estimation of the fault locations of the lateral feeders by short-circuit analysis is presented.. Another approach, unbalanced faults and impacts of photovoltaic (PV) was considered. The proposed procedure consists of two stages. In Stage 1, the fault location for the main feeder was estimated using PMUs installed at the start and end points of the main feeder. Symmetrical components of voltage and Current fluctuations were calculated taking into account, the effects of the PVs connected to the side feeds. If the result of Stage 1 indicated a connection section of the lateral feeder, Stage 2 will be performed. In Stage 2, the fault location was estimated for the lateral feeder by comparing the results of the short-circuit analysis and the PMU measurements. The short-circuit analysis was based on an unbalanced power flow that took into account the dynamic properties of the photovoltaic inverter. The proposed method was verified by various fault situations in a test system. A noise test was also performed for the applicability of the proposed algorithm to the actual system.

Introduction:

This is a method of estimating the fault location by combining the PMU measurements and contingency analysis results using short circuit calculation. To that end, this method proposes the following three points. First, a 2-stage fault location estimation method is proposed that identifies the fault location in the main feeder using two PMUs installed in the main feeder, and then compares the contingency short circuit analysis result and the PMU measurements to estimate the fault location inside the lateral feeder. Second, the existing method is modified, which only uses the positive sequence components of voltage and current without considering the contribution of DER, by proposing a method of calculating the voltage variation by decomposing voltage and current into symmetrical components. Furthermore, a method of combining the voltage phasor angle measurement of the PMU and the RTU measurement to reflect the fault current contribution of DERs to the main feeder is proposed. Third, to estimate the fault location in the lateral feeder, a short circuit analysis method is used that reflects the

dynamic control characteristics of the PV inverter during a fault for the implicit Z-bus method, which is a conventional 3-phase power flow method. In order to verify the applicability of the proposed algorithm to the actual system, a random noise test was performed.

Conventional Fault Location Methods Using PMUs:

The study assumed that every bus is a faulted point and calculated the current between buses by using the measurement values that were obtained by PMUs installed at the substation and DERs[2]. After that, the voltage of the PMU installation point was calculated through weighted least squares-based state estimation by using line impedance and calculated current. The fault location was identified through the comparison between the estimated and measured values of the voltage at the PMUs. As shown in Figure 1, if bus 4 is assumed as the fault point, the upstream current of the fault point is calculated by using the I1 and IDER1. If bus 6 is assumed as the fault point also, it is calculated with additional consideration for IDER2. The voltage is estimated for each case by using the calculated current and line impedance. If the case of the assumed fault at bus 4 has the smallest deviation (comparing with the estimated and measured voltages for each bus), it can identify the bus as the fault location. However, this method requires the installation of many PMUs at every DER point, at both ends and of the feeder, and in the middle of the feeder

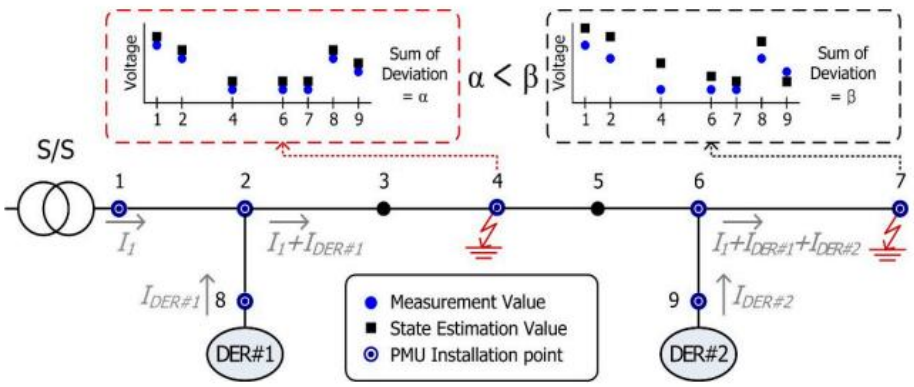

Figure 1. Outline of the phasor measurement unit (PMU)-based fault location method [redacted]

The study used the voltage and current variations before and after the fault detected at the PMUs[3]. For estimation of the fault location, the positive sequences of voltage and current variations were calculated for the forward (from start to end of a feeder) and backward (from end to start of the feeder) direction, as expressed by Equation (1) and (2).

$$\Delta I_n = \Delta I_{n-1} - \Delta V_{n-1} * Y_{n-1} \quad (1)$$

$$\Delta V_n = \Delta V_{n-1} - \Delta I_n * Z_{n,n-1} \quad (2)$$

where, ΔVn and ΔIn are the positive voltage and current variations of each bus n. For calculation of the variations in each direction, the measured values of the PMU are used as the initial value. Zn,n−1 is the line impedance between the bus n and n − 1. Yn−1 is the admittance of the load connected to the bus n − 1. Finally, the fault location was determined as a section where the voltage difference between the two directions was minimized as shown in Figure 2.

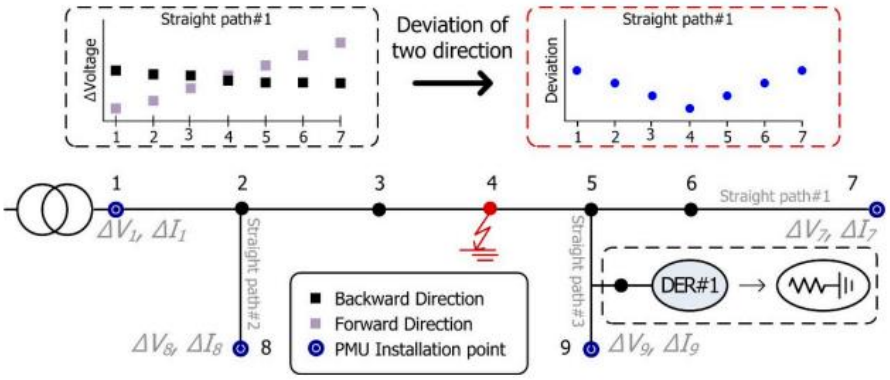

Figure 2. Outline of the PMU-based fault location method

This method calculated variation values using only the positive sequence. Therefore, it was required to consider the symmetrical components for the unbalanced faults. Additionally, the lateral feeders were treated as simply impedance model. It is can be erroneously calculated due to the contribution of the DERs connected to the lateral feeders. Above all, that requires two PMUs at both ends of the straight paths for a feeder to identify a fault in the main and every lateral feeder. Even for the reduction distribution network shown in Figure 2, as many as four PMUs are required. This will require the installation of much more PMUs for the actual distribution networks. According to other studies, the PMU can generate approximately 13 GB

of data every month[4-5]. Moreover, the generation of monthly communication costs will be at least $13.84 for each PMU, which aggravates the economic burden. Table 1 presents the amount of data required by each PMU installed in the distribution networks. Table 2 shows the corresponding cost of communication[4]. In Table 2, the use of wireless communication was assumed. Additionally, separate communication infrastructure and costs are required to use an optical network. Therefore, as the increase of PV connected to distribution network, installing many PMUs is not a practical solution to the fault location.

Table 1. Monthly amount of accumulated data for each terminal unit.

Type of Meter	RTU	PMU	Smart Meter
Amount of data/cycles	1/2 s	10–120 s	1/15 min
Acquisition data type	P, Q, V (m), I (m), θ_{V-I}, etc.	P, Q, V (m, δ), I (m, θ), etc	P, V, etc.
Accumulated data generation/month	*44.2 MB*	*1.13–13.45 GB*	*0.41 MB*
Required communication speed	132 bps	3.36–40.32 kbps	1.227 bps

Table 2. Communication cost for PMU data transfer ($/month).

Data Transfer Samples (s)		10	60	120
Type of communication	NB-IOT	83.91	562.17	1136.94
	LTE	13.84	13.84	20.77

The Proposed 2-Stage Fault Location Method:

The Proposed Fault Location Strategy

Figure 3 shows the overall strategy of the proposed fault location algorithm. The key of the proposed method is to minimize the number of PMU installations to two on the main feeder. For the minimization of the PMU installation, the fault location estimated for lateral feeders using the short circuit analysis instead of additional PMU installation. In this regard, it was assumed that two PMUs are installed at both ends of the main feeder and RTUs are installed at the start of the lateral feeders with large-capacity DERs. The three-phase active and reactive power of large-capacity DERs is also known by using the measurement unit. For the small-capacity DERs, the output ratio of large-capacity DERs was applied. It was assumed that the load is calculated by the conventional estimation method[1-6]. This assumed load value includes a certain amount of estimation error.

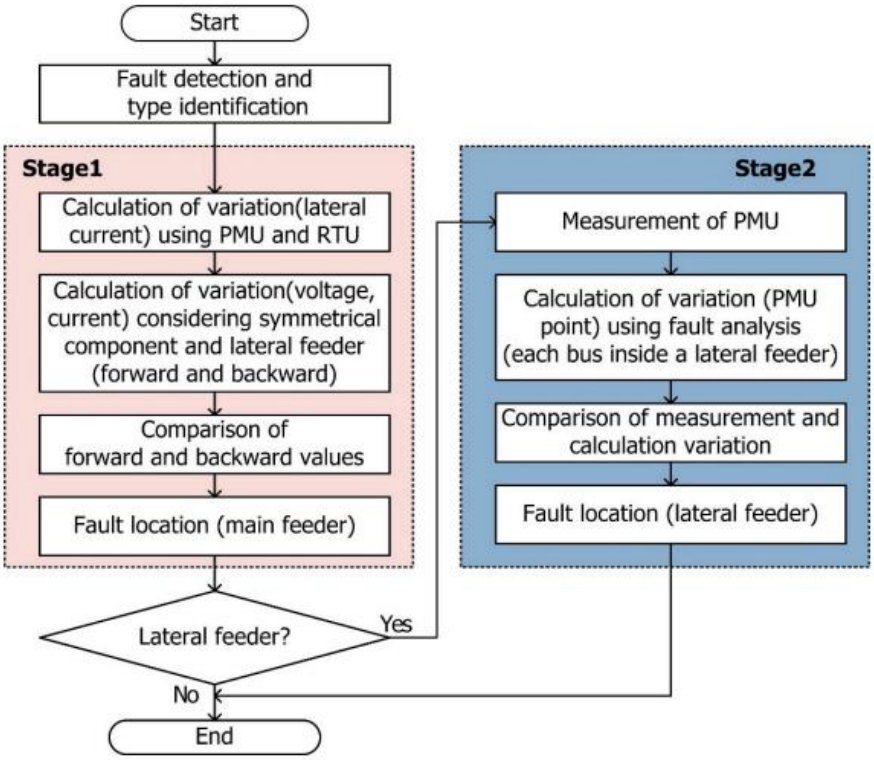

Figure 3. Overall flow chart of the proposed fault location method.

The proposed method consists of two stages. In Stage 1, the forward and backward methods expressed by Equations (1) and (2) above are applied[3]. Furthermore, the two problems for reference[3] were improved. Firstly, to consider the effect on the main feeder by the DERs connected to the lateral feeder, the current variation due to the DERs of the lateral feeder was calculated by using the PMU (voltage angles) and RTU (voltage–current angle difference and current magnitude) measurements. Secondly, to consider the unbalanced fault, the voltage variations in each direction were calculated by reflecting the symmetrical components. If Stage 1 estimated buses are connected to a lateral feeder, it is required to perform Stage 2 to estimate the fault location in the lateral feeder. On the other hand, the result of Stage 1 is determined as the final fault location. In Stage 2, a process is performed for the fault location estimation of a lateral feeder. The faults at each point in the lateral feeder were analyzed by using a short circuit analysis based on unbalanced power flow that considers the dynamic control characteristics of the PV inverter. Through the result of the short circuit analysis, the voltage and current variations were calculated at the PMU points. Finally, the calculated result and PMU measurements were

compared, and the two buses showing the smallest deviation between the two values were determined as the fault location.

Fault Detection and Identification

For the fault location, a preliminary stage of fault detection was necessary. This study conducted fault detection by utilizing existing PMU-based studies. The measurement characteristics of the PMU were utilized for fault detection. Through this, event detection was determined when the variation between samples increased remarkably. After that, the fault is detected when the measurement of voltage is lowered than a reference after event identification by setting the voltage reference about the fault[7]. In addition, in order to distinguish the types of fault, the reference values are set for the voltage variation in each phase at the PMU installation point. For example, if the voltage variation at each phase is uniform, this fault will be identified as a three-phase short circuit. If one phase has a large deviation from the other two phases, the fault will be identified as a single line-to-ground fault. Based on such a principle, fault types in a power system will be identified.[8]

Fault Location in the Main feeder: Stage 1

In Stage 1, to solve the problems of the previous study[3], there was the calculation of the effect of DER of the lateral feeder on the main feeder. Moreover, voltage and current variation were calculated by using symmetrical components to consider the unbalanced fault. RTU measurements at the start point of the lateral feeders with large-capacity DERs and PMU measurements at both ends of the feeder were used to calculate the impacts of DERs of lateral feeders on the main feeder. This method assumed that the voltage phasor is similar at upstream and downstream of the fault point in the distribution networks. Therefore, the impact of the DERs at the lateral feeder was calculated by replacing the voltage angle at the RTU installation point with the voltage angle at the PMU. To calculate the current variation due to the DERs of the lateral feeder, the current magnitude of the RTU, voltage angle (δ) of the PMU and angle difference ($\theta V-I$) between the voltage and current of the RTU data were utilized. The current variation of each phase by the lateral DERs was calculated as expressed in Equation (3).

$$\Delta I_{lateral}^{A;B;C} = I_{lateral_{post}}^{A;B;C} \angle\left(\delta_{V_{post}}^{A;B;C} - \theta_{V-I_{post}}^{A;B;C}\right) - I_{lateral_{pre}}^{A;B;C} \angle\left(\delta_{V_{pre}}^{A;B;C} - \theta_{V-I_{pre}}^{A;B;C}\right) \quad (3)$$

where $I^{A;B;C}_{lateralpost}$ and $I^{A;B;C}_{lateralpre}$ are the currents at each phase for before and after the fault, these are measured at RTU. $\delta^{A;B;C}_{Vpost}$ and $\delta^{A;B;C}_{Vpre}$ are the voltage phasor measured at the PMUs. $\theta^{A;B;C}_{V-Ipost}$ and $\theta^{A;B;C}_{V-Ipre}$ are the voltage–current phasor differences of each phase measured at RTU. In Equation (3) a slight error occurred compared with the actual measurement values because it is calculated by replacing the voltage angle. However, the fault current from the lateral feeder with DERs makes a smaller contribution than the substation. Therefore, it was judged that the small deviation generated by Equation (3) does not affect the estimation of fault location in the main feeder. The current variation of the buses in the main feeder was calculated by classifying the lateral and non-lateral buses, as expressed in Equation (4). In the case of the lateral feeder with only loads, the current variation is calculated for the form of concentrated load on the bus, as shown in the first term of Equation (4). For the lateral feeder with large-capacity DERs, it is calculated as the sum of the impact of DERs and current variation in the n − 1 bus

$$\Delta I_n^{A;B;C} = \left\{ \begin{array}{ll} \Delta I_{n-1}^{A;B;C} - \Delta V_{n-1}^{A;B;C} \times Y_{n-1} & if \quad n \notin \{k\} \\ \Delta I_{n-1}^{A;B;C} - \Delta V_{n-1}^{A;B;C} \times Y_{n-1} + \Delta I_{lateral}^{A;B;C} & else \quad n \in \{k\} \end{array} \right\} \quad (4)$$

where n denotes the number of each bus in the main feeder, and {k} is the set of buses next point of the lateral feeders. $\Delta V^{A;B;C}_{n-1}$ and $\Delta I_n^{A;B;C}$ are the voltage and current variations at each phase of bus in the main feeder. $\Delta I^{A;B;C}_{lateral}$ is the current variation at each phase in the lateral feeder. Finally, to calculate a voltage variation, the current variation is divided into positive, negative and zero sequence components, as expressed in Equation (5). After that, the voltage variation of the faulted phase is calculated by using Equation (6)

$$\begin{bmatrix} \Delta I_n^0 \\ \Delta I_n^1 \\ \Delta I_n^2 \end{bmatrix} = \frac{1}{3} \begin{bmatrix} 1 & 1 & 1 \\ 1 & \alpha & \alpha^2 \\ 1 & \alpha^2 & \alpha \end{bmatrix} \begin{bmatrix} \Delta I_n^A \\ \Delta I_n^B \\ \Delta I_n^C \end{bmatrix} \quad (5)$$

$$\Delta V_n^{faulted\ phase} = \Delta V_{n-1}^{faulted\ phase} - \Delta I_n^1 * Z_{n,n-1}^1 - \Delta I_n^2 * Z_{n,n-1}^2 - \Delta I_n^0 * Z_{n,n-1}^0 \quad (6)$$

where ΔV_n faulted phase denotes the voltage variations of each bus for a faulted phase before and after the fault. $\alpha = 1\angle 120^\circ$, ΔI^n_1 , ΔI^n_2 , and ΔI^n_0 are the symmetrical components of the current variation of each bus. $Z^1_{n,n-1}$, $Z^2_{n,n-1}$, and $Z^0_{n,n-1}$ are the symmetrical components of line impedance between the nth and n − 1th bus. Figure 4 shows the flowchart of Stage 1 considering the above improvements.

1. In order to estimate the fault location for the main feeder, the necessary data for Equation (3)–(6) were obtained through RTUs and PMUs.

2. The effect of DERs at a lateral feeder on the main feeder was calculated by using Equation (3). To calculate the effect of the lateral feeder of each direction, it was applied by replacing the voltage angle at the RTU installation point with the one at the PMU.

3. For the fault location in the main feeder, the voltage and current variations were calculated by forward and backward directions. Additionally, the buses of the main feeder were classified into non-lateral and lateral buses to calculate the current variations. Through this, voltage variations considering symmetrical components were calculated by using Equations (4)–(6).

4. Finally, the fault location in the main feeder was estimated by calculating the deviations of voltage variations between each direction, which are obtained in Step 3. The two buses with the smallest deviation were estimated as the fault location. If the estimated buses are connected to a lateral feeder, Stage 2 is required to estimate the fault location in the lateral feeder.

Fault Location in the Lateral Feeder: Stage 2

As mentioned in Figure 2, Stage 2 was performed when the estimated result of Stage 1 indicates buses connected to the lateral feeder. In Stage 2, each bus of the lateral feeder identified in Stage 1 was assumed for the faulted bus candidate. Then, the voltage and current variations after the fault occurrence at the installation points of the PMUs were calculated through the short circuit analysis for the candidate buses. Finally, the fault location in the lateral feeder was estimated by comparing the measured values from the PMU and calculated values. Therefore, this method requires a precise short circuit analysis that considers the dynamic characteristics of DERs during a fault and the unbalanced characteristics of the distribution network. In this method, the

characteristics of the PV inverter are considered, which occupies the largest proportion of the DER in the distribution networks.

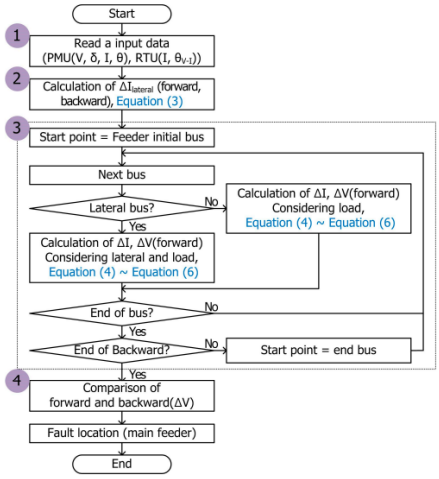

Figure 4. Flowchart of the proposed fault location method (Stage 1).

There are several methods for the control of PV output. In this method, the balanced positive sequence control (BPSC) is considered, which is one of the PV control methods[9]. For this method, the inverter of the PV is controlled as the three-phase balanced current according to the solar radiation and lowest voltage among the three-phases at the interconnected point of the inverter. The control characteristics of the PV inverter using BPSC are expressed by Equation (7).

$$S_{PV\_3Phase} = V_{PV\_A}\,(I_{PV\_A})^* + V_{PV\_B}\left(\alpha^2 I_{PV\_A}\right)^* + V_{PV\_C}(\alpha I_{PV\_A})^*\,[VA] \quad (7)$$

Where, $V_{PV\_A\ or\ B\ or\ C}$ is the voltage of each phase at the interconnection point of the PV. I_{PV_A} is the phase A current at PV. In Equation (7), the ratio of the PV output power for each phase can be expressed by Equation (8).

$$S_{PV\_A} : S_{PV\_B} : S_{PV\_C} = V_{PV\_A} : \alpha V_{PV\_B} : \alpha^2 V_{PV\_C} \quad (8)$$

where $S_{PV\_A\ or\ B\ or\ C}$ is the output power of each phase. Additionally, the PV inverter set a maximum current (usually 1.2–2 times the rated current) to prevent the internal circuit of the inverter from being damaged by an overcurrent[10]. If the output current of the inverter is below

the maximum current, it is controlled as a balanced current according to the solar radiation. Otherwise, the output current is controlled as a constant current source that is fixed to the maximum magnitude and angle of the PV inverter as shown in Equation (9)

$$I_{PV\_Phase} = \begin{cases} \frac{S_{PV\_Phase}}{V_{PV\_Phase}} & if \quad I_{PV} < I_{PV,\,max} \\ I_{PV,\,max} & else \quad I_{PV} \geq I_{PV,\,max} \end{cases} [A] \qquad (9)$$

Where, V_{PV_Phase} and I_{PV_Phase} are the phase current and voltage of the PV. I_{PV}, max denotes the maximum current of the inverter. S_{PV_Phase} is also the output power for each phase. As shown in Equation (8), S_{PV_Phase} is determined by the voltage of each phase at the PV interconnection point. Consequently, to estimate the fault location in the distribution networks, the short circuit analysis must consider the above-mentioned dynamic control characteristics of the PV inverters. Traditional short circuit analysis utilizing an impedance model and its symmetrical components cannot consider such dynamic characteristics. Accordingly, this method used a three-phase unbalanced power flow for the short circuit analysis considering the control characteristics of the PV inverter under fault conditions. For the unbalanced power flow, the implicit Z-bus method was applied, which is widely used in the distribution system[11]. This method determines a voltage by aggregating the variations of the current and voltage, which are attributable to the load and PVs in distribution networks and to the equivalent voltage source of a transmission system. As expressed by Equation (10), this method calculates the voltage variation for the impact of the equivalent source on the transmission networks.

$$V_{NL} = Z_{bus} I_{NL} \rightarrow \begin{bmatrix} V_{NL1} \\ V_{NL2} \\ \vdots \\ V_{NLn} \end{bmatrix} = Z_{bus} \begin{bmatrix} I_{NL1} \\ 0 \\ \vdots \\ 0 \end{bmatrix} [V] \qquad (10)$$

Where, V_{NL} is the voltage variation of each bus when the equivalent source of the transmission system is energized and all the loads and PVs in distribution networks are opened. For calculating the V_{NL2}–V_{NLn}, the admittance matrix and V_{NL1} (known value because this is the PMU measurement of the bus immediately before the fault) was used. In the next step, the

impact of the voltage source was excluded, and the PVs and loads in the distribution networks were treated as current sources. The voltage variation is calculated according to the impact of current sources, as expressed by Equation (11). The voltage of the buses was calculated by performing an iterative calculation because the PV output current is changed by its terminal voltage.

$$V_L{}^k = Z_{bus} I_L{}^{k-1} \rightarrow \begin{bmatrix} V_{L1}{}^k \\ \vdots \\ V_{Li}{}^k \\ \vdots \\ V_{Lj}{}^k \\ \vdots \\ V_{Ln}{}^k \end{bmatrix} = Z_{bus} \begin{bmatrix} 0 \\ \vdots \\ I_{Li}{}^{k-1} \\ \vdots \\ I_{Lj}{}^{k-1} \\ \vdots \\ 0 \end{bmatrix} [V] \qquad (11)$$

Where, V_L is the voltage variation caused by loads and PVs. I_L is the current variation affected by loads and PVs. k is the number of iterations. i, j, and n denote the number of each bus. Finally, as expressed in Equation (12), the voltage variation of every bus is calculated by aggregating the voltage variations by using Equations (10) and (11).

$$V_n{}^k = V_{NL} + V_L{}^k [V] \qquad (12)$$

Figure 5 shows the fault analysis algorithm based on a three-phase power flow, which considers the dynamic control characteristics of the PV.

1. In the first step of the short circuit analysis, the distribution network was divided into slack, load, and PV (generator) buses. The initial values, such as bus voltage, load, and reactive control method of the PV inverter, solar radiation, and transformer winding were acquired.

2. An admittance matrix for the short circuit analysis was composed based on the assumed faulted bus in the lateral feeder and identified fault type. To perform the three-phase power flow, the admittance matrix of a line was calculated through an impedance matrix from modified Carson's Equations by using the line diameter, each phase-to-phase distance, a line-to-ground distance and other data[12]. In the case of the three-phase 4-wire line network, a 3 × 3 matrix considering the impact of a neutral line was obtained by the Kron reduction. A three-phase

modeling of transformer was performed according to the connection types[13]. As shown in Equation (13), the faulted phase at the fault point was treated as connected to the earth or short-circuited to another phase.

$$Z_{f_{1\varnothing}} = \begin{bmatrix} Z_f & 0 & 0 \\ 0 & \infty & 0 \\ 0 & 0 & \infty \end{bmatrix}, \; Z_{f_{3\varnothing}} = \begin{bmatrix} Z_f & 0 & 0 \\ 0 & Z_f & 0 \\ 0 & 0 & Z_f \end{bmatrix}, \; Z_{f_{AB}} = \begin{bmatrix} Z_f & 0 & \infty \\ 0 & Z_f & \infty \\ \infty & \infty & \infty \end{bmatrix} \quad (13)$$

Where, Z_f is the resistance at the fault point, $Z_{f1\emptyset}$ is the single line-to-ground fault, $Z_{f3\emptyset}$ is the three-phase fault, and Z_{fAB} is the line-to-line fault between phases A and B. In this process, the components and fault points were considered as a three-phase impedance model, which was transformed into an admittance matrix for power flow. Figure 6 illustrates the admittance configuration. The final admittance matrix was composed of self-admittance and mutual admittance components. A 3 × 3 matrix was assigned to each bus, and the number of the rows and columns was three times the number of the buses.

3. To consider the dynamic characteristics of the PV inverter, the voltage and current variations were calculated by using Equation (10) for the equivalent source of a transmission system, and those by the PVs and loads were calculated by using Equation (11). The voltage of the PV interconnection point was estimated by aggregating the results by using Equation (12). If the calculated voltages did not converge or the calculated PV inverter current in Step 4 exceeded the maximum current, Step 3 was repeated by using the updated output current of the PVs.

4. The output current of the PV inverter was calculated by using Equation (9). The voltage of the PV interconnection point was also obtained by Step 3. If the calculated current was lower than the maximum current of the inverter, the convergence of the voltage was checked. If the voltage convergence did not occur, updating of the voltage and current of Step 3 was repeated. If the calculated output current of the PV also exceeded the upper limit of the inverter, the magnitude and angle were updated, and the voltage and current were updated in Process 3.

5. If the voltages converge, the short circuit analysis was not repeated. Then, the voltage and current variations at the installation point of the PMUs were calculated to apply the short circuit analysis result to the fault location of a lateral feeder (Stage 2).

Figure 7 shows the strategy for the estimation of fault location in Stage 2.

1. The voltage and current variations obtained through each PMU were stored.

2. The fault resistance is estimated. For this calculation, the lateral feeder that decided to the faulted section at the Stage 1 is divided into subsections, and fault analysis in Figure 6 is performed by varying the assumed fault resistance for each subsection. Consequently, the estimated fault resistance is determined by the comparison with the result of short circuit analysis and the measurement of PMU at the main feeder start point.

3. The voltage and current variations at the installation point of the PMUs were calculated through the short circuit analysis illustrated in Figure 5.

4. The sum of the absolute error was calculated for each bus by using Equation (14). Then, the two buses with the smallest result were selected as the fault location in the lateral feeder.

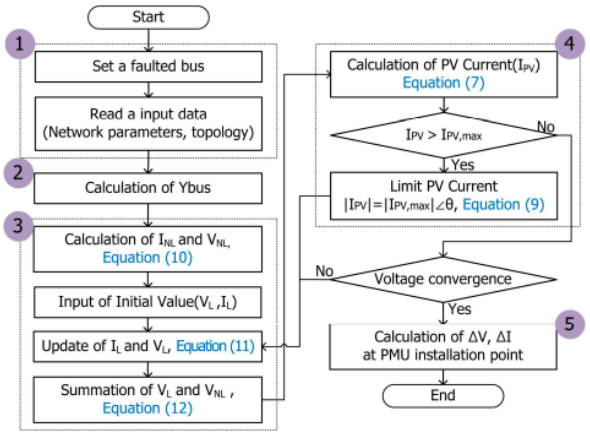

Figure 5. Flowchart of the dynamic fault analysis.

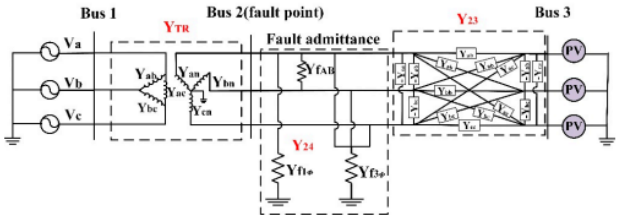

Figure 6. Three-phase admittance configuration of a distribution network under a fault.

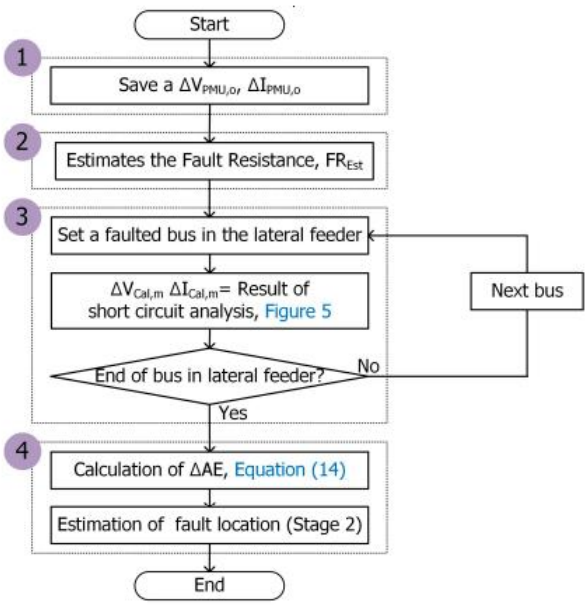

Figure 7. Flowchart of the proposed fault location method (Stage 2).

To estimate the fault location in the lateral feeder, the absolute error between the short circuit analysis result and PMU measurement was calculated using Equation (14). Here, the absolute error represents the difference between the voltage and current measurement variations of each PMU installation point and the variations of the PMU installation point obtained through short circuit analysis when a fault was assumed in each bus inside the lateral feeder. Therefore, for the fault location inside the lateral feeder, two buses, where the sum of these absolute errors becomes the smallest, were considered a faulted section inside the lateral feeder.

$$\Delta AE = \left|\Delta V_{\mathrm{PMU,\,o}} - \Delta V_{\mathrm{Cal,\,m}}\right| + \left|\Delta I_{\mathrm{PMU,\,o}} - \Delta I_{\mathrm{Cal,\,m}}\right| + \left|\Delta \delta_{\mathrm{PMU,\,o}} - \Delta \delta_{\mathrm{Cal,\,m}}\right| + \left|\Delta \varphi_{\mathrm{PMU,\,o}} - \Delta \varphi_{\mathrm{Cal,\,m}}\right| \quad (14)$$

where o is the number of PMUs, and m is the number of buses in the lateral feeder for which a fault is simulated. ΔV_{PMU} and ΔV_{Cal} indicate the measurement and the calculation of voltage magnitude variation, ΔI_{PMU} and ΔI_{Cal} denote the measurement and the calculation of current magnitude variation. $\Delta\delta$ and $\Delta\phi$ represent the variations of voltage and current phasor angle. If the estimated fault resistance (FR_{Est}) is below a certain value and there is an error in the measured value, due to the difference between the fault resistance and the impedance of lateral feeder is small, lots of errors can occur in the phasor angle calculation. In this case, since the

fault resistance is small and the magnitude of the fault current is relatively large, the absolute error can be calculated using only the initial two terms (comparison with voltage and current magnitude) of the Equation (14)

Case Studies:

To verify the proposed method, case studies were performed through various fault simulations by using Matlab Simulink. Figure 8 presents the single line diagram of the test system. As previously mentioned, it was assumed that two PMUs are installed at both ends of the main feeder and RTUs are installed at the start of the lateral feeders with large-capacity DERs. A feeder #5 of KADTS (Korea active distribution test system) was used for case studies. The model was developed for technical testing of active distribution networks using standard model data from KEPCO (Korea Electric Power Corporation) [14]. The feeder was applied for a medium-long length line. The length of each section was 0.8 km, and the total distance of the line was 20 km. The positive and negative sequence components (Z1 = Z2 = 3.47 + j7.57%) and a zero sequence component (Z0 = 8.71 + j22.84%) per km are applied by utilizing the impedance of ACSR 160/90 mm2 cables. In Figure 8b, the 'Lat' is the virtual bus at the connection point of the lateral feeder and it was used to estimate the fault location on the main feeder. The 'Lat' bus was assumed to exist on both sides of the 20 m from the lateral feeder connected bus. The test system based voltage was 22.9 kV lines. Each section load applied was also 250 kW. Table 3 presents the PV capacities in the test system. The PV1, 3, and 6 assumed that the measurement unit was installed.

Table 3. Set values for photovoltaics (PVs).

Type	PV1	PV2	PV3	PV4	PV5	PV6
Capacity	0.5 MVA	0.1 MVA	2 MVA	0.1 MVA	0.2 MVA	1 MVA
Maximum current/Rated current	1.2	1.2	1.2	1.2	1.2	1.2
Transformer	Yg/Yg	Yg/△	Yg/△	Yg/Yg	Yg/Yg	Yg/△
Capacity type	Large	Small	Large	Small	Small	Large

Figure 9 shows the PV system that is modeled on Simulink. The PV system was implemented through the consideration of the characteristics for the PV inverter. The PV system includes modules that enabled a user to limit the PV current inside an inverter. The control method of the inverter adopted the BPSC. Figure 9 shows the current and voltage of a PV system implemented

under a single line-to-ground fault. It can be seen that in the case of a fault, the current is controlled in balanced, and the voltage changes by the fault type.

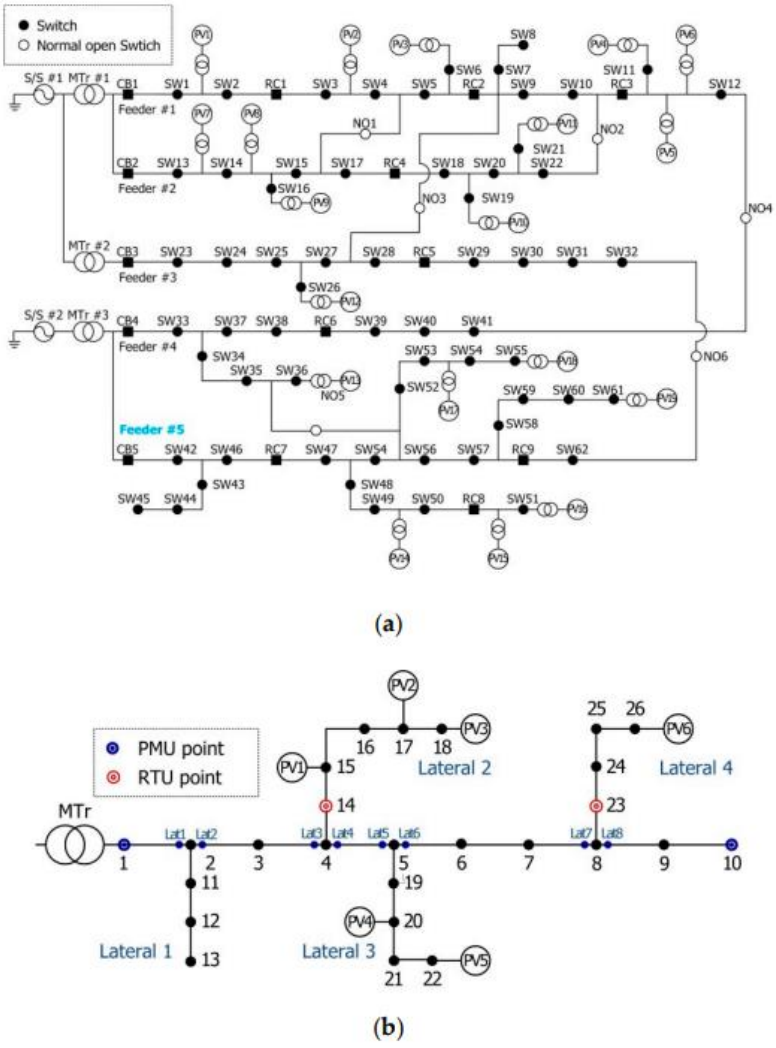

Figure 8. Test system for the case studies. (**a**) Test model of the Korea active distribution test system (KADTS). (**b**) Modified test system.

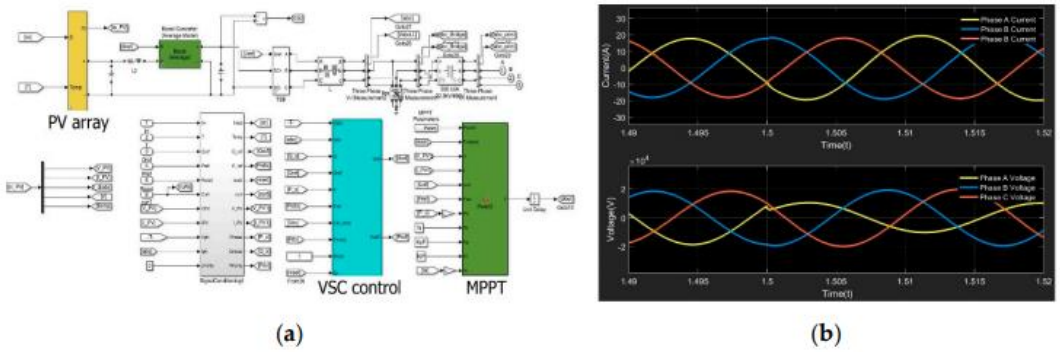

(a) (b)

Figure 9. Modeling of a PV system. (**a**) PV system in Simulink. (**b**) PV control characteristics in the fault condition.

Fault Location Estimation in the Main feeder

Comparative Analysis of the Conventional Method:

To verify the algorithm of Stage 1, a single line-to-ground fault was simulated for Buses 7 and 8 among the buses in the main feeder. Table 4 presents the voltage variations and calculation results for each bus obtained in Stage 1. A "FWD" and "BWD" denote the voltage variations that were calculated at the start and end PMUs in the forward and backward directions. "DEV" means the deviation of calculations between the FWD and BWD. The results in Table 4 show that the proposed method was approximately the same as the Matlab simulation results and the estimated fault location was accurate. The W/O (without) PV was calculated without considering the impact of the PV in the lateral feeder. The W/O PV results had an erroneous fault location because the calculation error occurred after the lateral feeder due to the impact of PV. In the existing method, it could be seen that a large error occurred because the symmetrical component and impact of the PV was not considered[3]. As a result, the fault location was estimated to be between Buses 9 and 10 that were completely different from the actual fault location. The bottom part of Table 4 shows the comparison with the calculation and simulation results for the current impact of the lateral feeders.

Table 4. Comparison of fault location results under a single line-to-ground fault.

Variation of Bus		ΔV_1	ΔV_2	ΔV_3	ΔV_4	ΔV_5	ΔV_6	ΔV_7	ΔV_8	ΔV_9	ΔV_{10}
Proposed Method	FWD	0.297	0.389	0.483	0.578	0.687	0.796	0.905	1.015	1.140	1.264
	BWD	1.134	1.106	1.079	1.052	1.036	1.022	1.007	0.993	0.993	0.993
	DEV	0.849	0.724	0.601	0.477	0.352	0.228	0.104	0.025	0.147	0.272
Proposed Method (W/O PV)	FWD	0.297	0.389	0.483	0.578	0.674	0.771	0.867	0.964	1.061	1.158
	BWD	0.998	0.997	0.996	0.995	0.994	0.994	0.993	0.993	0.993	0.993
	DEV	0.714	0.616	0.518	0.420	0.323	0.225	0.128	0.031	0.068	0.165
Method in [12]	FWD	0.297	0.359	0.422	0.486	0.551	0.616	0.682	0.748	0.814	0.881
	BWD	0.997	0.996	0.995	0.994	0.994	0.993	0.993	0.993	0.993	0.993
	DEV	0.712	0.646	0.579	0.512	0.446	0.379	0.312	0.245	0.179	0.112
Matlab Simulation		0.297	0.390	0.484	0.579	0.688	0.798	0.908	0.993	0.993	0.993

Lateral / Type	$\Delta I_{lateral2}^{faulted\ phase}$		$\Delta I_{lateral4}^{faulted\ phase}$	
	ΔI	$\Delta\varphi$	ΔI	$\Delta\varphi$
Proposed Method	0.0669	147.1615	0.0758	137.5514
Matlab Simulation	0.0667	148.0101	0.0758	137.4807

Notes: The shaded parts in Table 4 show the estimated fault section for each method.

Figure 10 shows the results of the proposed algorithm under the fault of the main feeder. The actual fault location is marked in the red line, while the method result is marked in the orange line[3]. As shown in Figure 10, the proposed method calculated approximately the same results in the Matlab simulation. Consequently, the proposed method accurately identified the actual fault location. The existing study did not consider the impact of the PVs and symmetrical components in the unbalanced faults, except the short circuit faults such as Figure 10c,d. Therefore, In Figure 10a,b, it could be confirmed that there was an error in estimating the fault location.

Stage 1 Estimation Results for the Error Test:

To verify the robustness of the proposed method, simulations were performed for the error of network models and measurements. In the case of the network model, the proposed method could be affected by the error of the line parameters and the load estimation value. However, line parameter error (line length, phase information, etc.) was excluded from this nethod because it was considered an improvement point of the utility's operation and maintenance. To verify the effect of the load, the single line-to-ground fault with 30 Ω was simulated, and 1000 simulations were conducted for each fault location. Cases 1–3 include the error of 5%, 10%, and 15%, respectively. Table 5 shows the simulation results for the main feeder according to the load errors. It estimated a fault location to 100% in all cases. Various load estimation methods were proposed, as the Ref[1]. Therefore, it was considered that the occurrence of a slight error by load estimation methods would not be a big problem in the application of the proposed method.

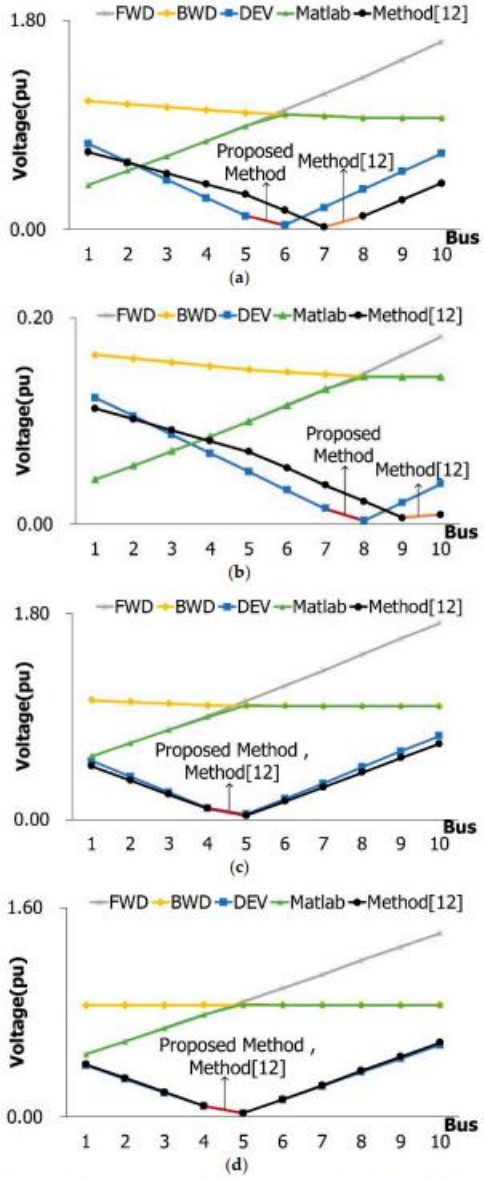

Figure 10. Fault location results under a fault in the main feeder, (**a**) single line-to-ground between Buses 5 and 6, (**b**) single line-to-ground between Buses 7 and 8 (resistance of fault point is 30 Ω), (**c**) Line-to-line between Buses 4 and 5, and (**d**) three-phase fault between Buses 4 and 5.

Table 5. Accuracy of the fault location according to load errors (fault in the main feeder).

Cases / Fault Location	Case1	Case 2	Case 3
	5%	10%	15%
	Stage1	Stage1	Stage1
2–3	100%	100%	100%
4–5	100%	100%	100%
6–7	100%	100%	100%
7–8	100%	100%	100%

Moreover, the robustness of the proposed method was verified for the measurement errors that could occur in the actual operation. The measurement error test was performed by applying noises to the voltage and current magnitudes of the RTU and PMU and the phasor angle measurements of the PMU. In Table 6, random errors were applied to the PMU and RTU measurement values (voltage and current magnitude) by protection class 3 specified by IEEE C57.13 and IEC 61869[24-25]. The phasor angle errors of a voltage and current were also applied to the PMU by C37.118[13]. For random error tests, a standard normal distribution was used. The range of standard deviation 3σ was applied to the error tests. The single line-to-ground fault was simulated, and 1000 simulations were conducted for each fault location. Cases 1–4 include the fault resistances of 0, 10, 20, and 30 Ω, respectively. The simulated fault locations were as follows: between Buses 2–3, 4–5, 6–7, and 7–8.

Table 6. Accuracy of the fault location according to measurement noises (fault in the main feeder).

Type / Fault Location	Case1	Case 2	Case 3	Case 4
	0 Ω	10 Ω	20 Ω	30 Ω
	Stage 1	Stage 1	Stage 1	Stage 1
2–3	100%	100%	100%	100%
4–5	100%	100%	100%	99.2%
6–7	100%	100%	100%	100%
7–8	100%	100%	100%	99.1%

Although there were slight errors when the fault resistance was above 30 Ω, the accuracy of fault location was 100% for almost cases. Therefore, it was confirmed that it is robust to the measurement error of Stage 1. To verify the effect of the phasor angle error of a voltage and current measurement for PMUs during the main feeder fault, the case studies were performed based on Case 1 (0 Ω), which had the most volatile voltage and current variation among the above cases. Cases 1–4 added the phasor angle error of 0.57◦, 1◦, 2◦, and 3◦ respectively. Table 7 shows the test results for the main feeder based on phasor angle errors. As a result, slight errors were recorded when the phasor angle error was above 3◦, but the accuracy of fault location was almost 100% for all cases. Therefore, it was confirmed that the phasor angle error did not have a significant effect for fault location estimation of the main feeder.

Table 7. Accuracy of the fault location according to phasor angle error (fault in the main feeder).

Type / Fault Location	Case1	Case 2	Case 3	Case 4
	0.57°	1°	2°	3°
	Stage 1	Stage 1	Stage 1	Stage 1
2–3	100%	100%	100%	100%
4–5	100%	100%	100%	99.8%
6–7	100%	100%	100%	100%
7–8	100%	100%	100%	99.9%

Fault Location Estimation in the Lateral Feeder

Analysis of the Short Circuit Analysis Results:

Table 8 presents the comparison results between the Matlab simulation results ("M") and proposed short circuit analysis results ("C"). The single line-to-ground fault was simulated at every bus in the test system. The voltage and current values after the fault at the PMU points were comparatively analyzed. At the start and end of the feeder, the voltage and current were calculated at an error rate of approximately below 0.01%. Consequently, the proposed short circuit analysis method could calculate the variations of each bus before and after a fault, which were sufficiently applicable to the fault location in the lateral feeder

Table 8. Comparison between the fault analysis and Matlab simulation.

Type / Bus		4		8		11		21		24	
		Mag. (A)	Ang. (Deg)	Mag. (A)	Ang. (Deg)	Mag. (A)	Ang. (Deg)	Mag. (A)	Ang. (Deg)	Mag. (A)	Ang. (Deg)
M	V_{PMU1}	6777.2	18.84	9531.3	23.68	5719.5	17.46	9695.2	23.92	10146.0	24.74
C	V_{PMU1}	6766.0	18.63	9522.8	23.56	5712.0	17.23	9687.1	23.81	10139.6	24.65
Error (%)		0.002	0.011	0.001	0.005	0.001	0.013	0.001	0.005	0.001	0.004
M	V_{PMU2}	634.3	26.60	5.60	98.78	3947.9	21.29	4893.2	24.65	2342.8	25.43
C	V_{PMU2}	627.1	26.75	5.49	100.01	3928.7	20.95	4882.8	24.52	2339.8	25.32
Error (%)		0.011	0.006	0.020	0.012	0.005	0.016	0.002	0.005	0.001	0.004
M	I_{PMU1}	4258.3	−47.53	2471.3	−43.20	4916.3	−49.58	2365.4	−42.86	2065.4	−42.25
C	I_{PMU1}	4272.5	−48.55	2483.8	−44.13	4928.9	−50.63	2377.1	−43.77	2075.9	−43.17
Error (%)		0.003	0.021	0.005	0.022	0.003	0.021	0.005	0.021	0.005	0.022
M	I_{PMU2}	0.30	26.60	0.0027	98.76	1.88	21.29	2.33	24.65	1.12	25.43
C	I_{PMU2}	0.30	26.75	0.0026	100.01	1.87	20.95	2.33	24.52	1.12	25.32
Error (%)		0.000	0.006	0.037	0.013	0.005	0.016	0.000	0.005	0.000	0.004

Estimation Result of Stage 2:

To verify the proposed algorithm of Stage 2, the faults were simulated for the lateral feeder. Figure 11 shows the results of fault location. Figure 11a,c,e shows the estimation results of Stage 1. In Figure 11b,d,f, ΔAE denotes the sum of absolute errors by using Equation (14). ΔI_PMU and ΔV_PMU, Δδ_PMU, Δϕ_PMU are absolute errors between the calculated and measured values. ΔI_PMU2 is close to zero because it only affected by the load at the downstream of the PMU installation point. The fault simulation results demonstrated that Stage 1 estimated accurate fault locations for buses connected to the lateral feeder in every case. For calculation of the absolute errors in (14), if the estimated faulted resistance is less than 5 Ω, only the magnitude comparison is used. And in cases of more than 5 Ω, the entire Equation (14) is used. The criteria of fault resistance can be determined by short circuit analysis before applying the proposed algorithm to the target networks. In the case of Figure 11b,f, the magnitude comparison is only used because the estimated fault resistance is 0.065 Ω, 0.11 Ω, respectively. Through these results, it can be confirmed that the faulted section is accurately estimated because the magnitude deviation between buses is large when the fault resistance is small. In the case of Figure 11d, it can be seen that the magnitude and the phasor angle are compared because the estimated fault resistance is 29.875 Ω. The faulted section is accurately estimated according to the phasor angle deviation between buses. Therefore, it is necessary to consider not only the magnitude but also the phasor angle when a large fault resistance is inserted. As a result, Stage 2 confirms the accurate identification of the faulted sections in the lateral feeder

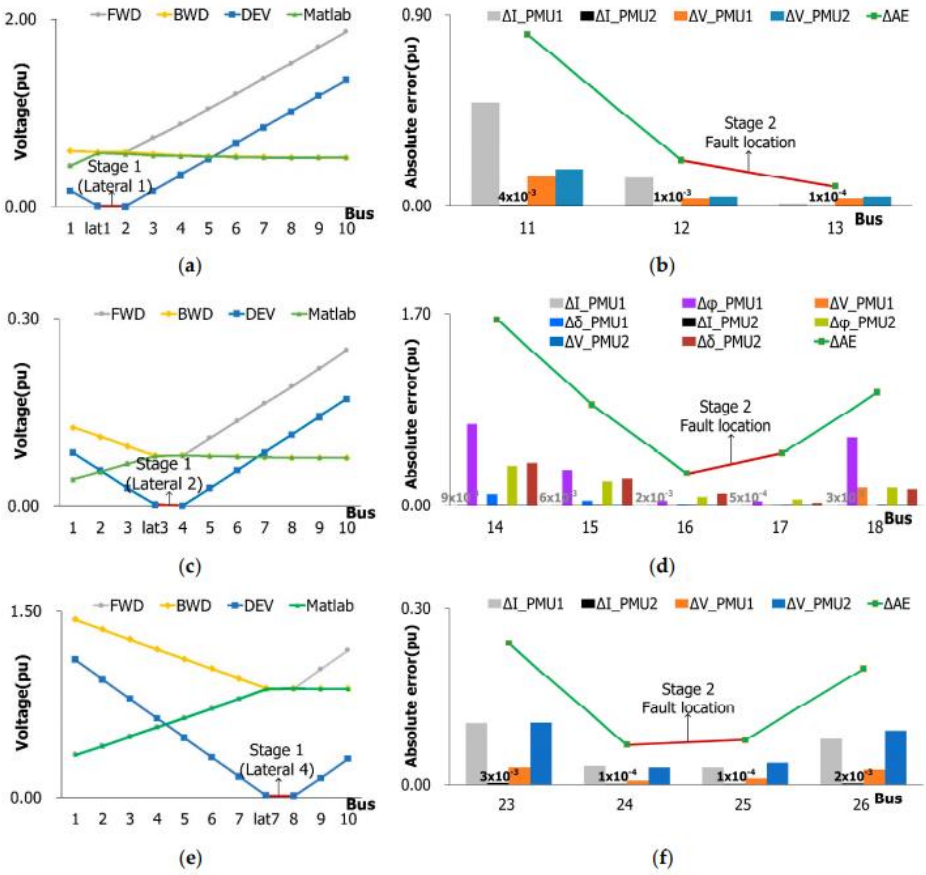

Figure 11. Results of fault location for the single line-to-ground fault between Buses 12 and 13, (**a**) Stage 1 and (**b**) Stage 2, result of fault location for single line-to-ground fault between Buses 16 and 17 (30 Ω), (**c**) Stage 1 and (**d**) Stage 2, result of fault location for three-phase fault between Buses 24 and 25, (**e**) Stage 1 and (**f**) Stage 2.

Stage 2 Estimation Results for the Error Test:

To verify the effect of Stage 2 for the load error, the same error test as the main feeder was conducted. Table 9 shows the results of the fault location for the lateral feeder according to the load errors. The proposed method estimates a fault location to 100% in all cases for the lateral feeder. As a result, the error of the load did not significantly affect the proposed method.

Table 9. Accuracy of the fault location according to load errors (faults in lateral feeder).

Error / Fault Location	Case 1		Case 2		Case 3	
	5%		10%		15%	
	Stage 1	Stage 2	Stage 1	Stage 2	Stage 1	Stage 2
11–12	100%	100%	100%	100%	100%	100%
17–18	100%	100%	100%	100%	100%	100%
20–21	100%	100%	100%	100%	100%	100%
23–24	100%	100%	100%	100%	100%	100%

Moreover, to verify the robustness of the algorithm against random measurement errors caused by a fault in a lateral feeder. The measurement error test was also performed by applying noises to the voltage and current magnitudes of the RTU and PMU and the phasor angle measurements of the PMU for the main and lateral feeder. The single line-to-ground fault was simulated between buses 11–12, 17–18, 20–21, and 23–24. Table 10 presents the noise test results. In Stage 1, the accuracy of the fault location was near 100% because the fault within a lateral feeder shows the same phenomenon as that of the fault in the connection point of the lateral feeder. In the test results of Stage 2, the accuracy of fault location was approximately 100% when the fault point resistance was below 20 Ω. The minimum accuracy of fault location was 97.6% when a fault includes the fault point resistance of 30 Ω. Case 4 has an insignificant current and voltage of magnitude and phasor angle deviations between the buses under the fault condition. Accordingly, the measurement noise as more influential in Case 4 than in other cases. However, the main feeder buses connected with the lateral feeder that occurred in the error of estimation were identified to be close to 100% by Stage 1. It will not be an important problem because the distance of the lateral feeder is short when the restoration of actual distribution networks.

Table 10. Accuracy of fault location according to the measurement noises (faults in lateral feeder).

Case / Fault Location	Case 1		Case 2		Case 3		Case 4	
	0 Ω		10 Ω		20 Ω		30 Ω	
	Stage 1	Stage 2	Stage 1	Stage2	Stage 1	Stage 2	Stage 1	Stage 2
11–12	100%	100%	100%	100%	100%	100%	100%	98.8%
17–18	100%	100%	100%	100%	100%	100%	100%	99.7%
20–21	100%	100%	100%	100%	100%	100%	100%	97.6%
23–24	100%	100%	100%	100%	100%	100%	100%	98.4%

Table 11 shows the result of the fault location when additional PMU was installed in the lateral feeder 3. As a result, the fault location result was estimated to be close to 100% for the lateral feeder 3. Therefore, the number of PMUs was reduced compared to the existing method, and a similar effect could be obtained when additional PMUs were installed only in the lateral feeder having a low fault location estimation rate.

Table 11. Accuracy of fault location according to the installation of PMU in the lateral feeder 3.

Case / Fault Location	Case 1		Case 2		Case 3		Case 4	
	0 Ω		10 Ω		20 Ω		30 Ω	
	Stage 1	Stage 2	Stage 1	Stage 2	Stage 1	Stage 2	Stage 1	Stage 2
20–21	100%	100%	100%	100%	100%	100%	100%	100%

To verify the effect of the phasor angle error for the lateral feeder, the same phasor angle error test conducted. Table 12 shows the phasor angle error test results for the lateral feeder. As shown in Table 12, 2◦ or higher phasor angle errors began to influence the faulted section estimation result. However, this will not be a problem when applying the proposed algorithm because the maximum phasor angle error is 0.57◦ in Ref[4-17], which is the specification of a commercial PMU product.

Table 12. Accuracy of fault location according to the phasor angle error (faults in lateral feeder).

Case / Fault Location	Case 1		Case 2		Case 3		Case 4	
	0.57°		1°		2°		3°	
	Stage 1	Stage 2	Stage 1	Stage 2	Stage 1	Stage 2	Stage 1	Stage 2
11–12	100%	100%	100%	100%	100%	100%	100%	100%
17–18	100%	100%	100%	100%	100%	100%	100%	100%
20–21	100%	100%	100%	100%	100%	100%	98.9%	97.9%
23–24	100%	100%	100%	100%	100%	100%	99.1%	95.7%

Conclusions:

To improve the excessive installation of PMUs, which is a common problem of existing PMU-based fault location methods, this study proposed a 2-stage fault location estimation method that combined the PMU measurements and short circuit analysis. In Stage 1 of the fault location in the main feeder, the symmetrical components of the voltage and current variations were

considered to deal with the unbalanced fault. It also considered the impact of the lateral feeder with large-capacity DER on the main feeder. In Stage 2 of the fault location in a lateral feeder, the faults at each point in the lateral feeder were analyzed by using a short circuit analysis based on the unbalanced power flow that considers the dynamic control characteristics of the PV inverter. Then, the short circuit analysis results were compared with the measurement values at the installation point of PMU. As mentioned above, the proposed method requires the simultaneous measurement of PMU installed points (both ends of the main feeder and additional points as needed). This is common to Stage 1 for fault location estimation in the main feeder and Stage 2 for comparing the short circuit analysis value and the measurement. Accordingly, the PMU was used because simultaneous measurements require the voltage, current, and phasor angle. The PQ meter or other instruments can also be used if they satisfy this requirement.

The following conclusions on the proposed algorithm were derived.

(1) The results of stage 1—where the fault location was simulated under diverse fault situations in the main feeder—were very similar to the Matlab simulation results. As compared with the existing study[3], the fault location was more accurate. Accordingly, the proposed method proved to be more effective as it considered unbalanced faults and the impact of DERs in the lateral feeder.

(2) In the results of Stage 2, it was confirmed that two buses with the smallest deviation between the short circuit analysis results considering the dynamic characteristics of the PV inverter and measured value of PMU were identified as the fault locations. Accordingly, unlike the existing PMU-based fault location methods, the proposed algorithm did not require the installation of additional PMUs and prevented an excessive number of PMUs from being installed in the distribution networks.

(3) To verify the robustness of the proposed method, simulations were performed for the error of network models and measurements. In the case of the network model, it was believed that the elements of the parameter errors that influence the proposed method are line parameters and load estimation data. The errors of the line parameters such as line length and phase are expected to influence every system analysis method and operation algorithm. However, this should be

researched as a separate topic because the line parameter errors are considered an improvement point of the utility's operation and maintenance. In recently, the grid modernization and the introduction of new operating system (advanced DMS) due to the increased complexity of the distribution network are promoting the correction of line parameter errors. When using the RTU as in this study, load values can be estimated more accurately by the RTU measurement and state estimation as shown in the Ref[1]. Moreover, as shown in the results of case study by load estimation error in Tables 5 and 9 in this study, the proposed method shows robust results even in load values with a 15% error. Therefore, it was believed that the load estimation error will not be a problem in applicability of the proposed method. The test of measurement errors was performed by applying noises to the voltage and current magnitudes of the RTU and PMU and the phasor angle measurements of the PMU. The magnitude and phasor angle errors were applied based on the standard and product specifications of Ref[4] and [15-17] For random error tests, the standard normal distribution that has the range of standard deviation 3σ was applied. In the measurement noise test, every fault case for the main feeder showed an accuracy of approximately 100%. In the fault cases of the lateral feeder, the accuracies were about 100% when the fault point resistance was 20 Ω and below. The fault location was identified with a minimum accuracy of 97.6% when the fault point resistance was 30 Ω. This can be seen to occur because the deviation for the magnitude of voltage and current and phasor angle between the buses was very small due to the fault resistance. However, the main feeder connected buses with the lateral feeder performed an estimation close to 100%. This will not be a big problem because the distance of the lateral feeder is short when there is restoration of the actual distribution networks. The fault location result is also estimated to be close to 100% for the lateral feeder 3 when additional PMU is installed at the end of lateral feeder 3. Therefore, the number of PMUs is reduced compared to the existing method, and similar effects can be obtained when additional PMUs are installed only in the lateral feeder having a low fault location estimation rate. As shown in the test results for phasor measurement error, 2◦ or higher phasor angle errors influenced the fault location estimation result. However, this will not be a problem when applying the proposed algorithm because the maximum measurement error of phasor angle is 0.57◦ in Ref[4-17], which is the specification of a commercial PMU product.

(4) The most remarkable advantage of the proposed method can be summarized as follows. The existing studies require the installation of many PMUs to estimate the impact of PVs and a fault location in the lateral feeder. The proposed method can achieve the same effect by using two PMUs at the main feeder, the RTUs, and the short circuit analysis method. The installation of additional PMUs causes a communication cost and infrastructure burden for the operation of distribution systems. As pointed out above, the proposed method will reduce the communication cost and accomplish accurate fault locations. These are significant improvements. Two problems that are worthy of notice still exist. First, the distribution networks are regularly reconfigured once or twice a year to ensure a load balance in each season and secure fault restoration reserves. For this reason, the locations of the PMUs installed at both ends of the main feeder may change. However, if the change of the PMU installation point from the reconfiguration of the distribution network may be excluded, the proposed method is sufficiently applicable to the actual distribution network. Second, the proposed method estimates the fault location by adding minimum PMUs in an existing network where RTUs are installed. Therefore, the proposed method can be applied to the systems where automation of the distribution system is applied (urban systems in Asia (including South Korea, Japan, Hong Kong, Singapore, etc.), Europe, and North America). However, it was assumed that the installation of RTUs for large capacity DER (such as PV), and applied the output ratio of large-capacity PV for small-capacity PVs. Hence, the cost can be increased by the installation of additional RTUs. However, this additional cost can be sufficiently covered by the actual operation because: (1) The PV output has a significant effect on the voltage and other problems recently in the operation of the distribution network. Therefore, the measurement of PV output is increasingly important for real-time operation of the distribution network (monitoring and control) and for establishing operation planning through PV output prediction. (2) The range of fault location can be reduced from the section with remote controlled switch to the section with manual switch. Furthermore, the fault location can be identified through data transfer between PMUs, which has the advantage of shortening the isolation time of the faulted section and the restoration time of the un-faulted sections. As mentioned above, the grid modernization and the introduction of new operating system also justify the additional installation of these new measuring devices. Additionally, according to IEEE 1547[18], DER is tripped after a voltage abnormally is detected for anti-islanding. This standard specifies the minimum trip time as 0.16 s (10 cycles). However, the PV trip will not

have a significant effect because the faulted section estimation using the PMU measurements uses measurements of much faster time than the time mentioned above. The management of distribution networks becomes a more complicated task due to the DERs. The improvement in reliability is one of the essential purposes for managing a distribution network. If the results of this study are utilized for network restoration in association with the distribution network management or for the agent-based fault recovery through device-to-device communication the reliability of distribution network will be more significantly improved than before.

Bibliography:

1. Fault Location Method Using Phasor Measurement Units and Short Circuit Analysis for Power Distribution Networks by Ji-Song Hong , Gi-Do Sim , Joon-Ho Choi , Seon-Ju Ahn and Sang-Yun Yun. Department of Electrical Engineering, Chonnam National University 77, Yongbong-Ro, Buk-Gu, Gwangju 61186, Korea; lklklkqaz@naver.com (J.-S.H.); rleh92@naver.com (G.-D.S.); joono@chonnam.ac.kr (J.-H.C.); sjahn@chonnam.ac.kr (S.-J.A.) Correspondence: drk9034@jnu.ac.kr; Tel.: +82-62-530-1745; Fax: +82-62-530-1749
2. Yun, S.-Y.; Chu, C.-M.; Kwon, S.-C.; Song, I.-K.; Choi, J.-H. The development and empirical evaluation of the Korean smart distribution management system. Energies 2014, 7, 1332–1362. [CrossRef]
3. Usman, M.U.; Faruque, O. Validation of a PMU-based fault location identification method for smart distribution network with photovoltaics using real-time data. IET Gener. Transm. Dis. 2018, 12, 5824–5833. [CrossRef]
4. Farajollahi, M.; Shahsavari, A.; Stewart, E.M.; Mohsenian-Rad, H. Locating the source of events in power distribution systems using micro-PMU data. IEEE Trans. Power Syst. 2018, 33, 6343–6354. [CrossRef]
5. IEEE. Standard for Synchrophasor Data Transfer for Power Systems; IEEE: Piscataway, NJ, USA, 2011.
6. Available online: www.powerstandards.com/wp-content/uploads/dlm_uploads/2017/10/Introduction-tomicroPMU.pdf (accessed on 18 February 2020).
7. Park, J.-Y.; Jeon, C.-W.; Lim, S.-I. Accurate section loading estimation method based on voltage measurement error compensation in distribution systems. J. Korean Inst. Illum. Electr. Install. Eng. 2016, 30, 43–48.

8. Biswal, M.; Brahma, S.M.; Cao, H. Supervisory protection and automated event diagnosis using PMU data. IEEE Trans. Power Deliv. 2016, 31, 1855–1863. [CrossRef]
9. Liang, X.; Wallace, S.A.; Nguyen, D. Rule-based data-driven analytics for wide-area fault detection using synchrophasor data. IEEE Trans. Ind. Appl. 2017, 53, 1789–1798. [CrossRef]
10. Castilla, M.; Miret, J.; Sosa, J.L.; Matas, J.; de Vicuna, L.G. Grid fault control scheme for three-phase photovoltaic inverters with adjustable power quality characteristics. IEEE Trans. Ind. Electron. 2010, 25, 2930–2940. [CrossRef]
11. Plet, C.A.; Green, T.C. Fault response of inverter interfaced distributed generators in grid connected applications. Electr. Power Syst. Res. 2014, 106, 21–28. [CrossRef]
12. Chen, T.H.; Chen, M.S.; Hwang, K.J.; Kotas, P.; Chebli, E.A. Distribution system power flow analysis a rigid approach. IEEE Trans. Power Deliv. 1991, 6, 1146–1152. [CrossRef]
13. Kersting, W.H. Distribution System Modeling and Analysis, 2nd ed.; CRC Press: Boca Raton, FL, USA, 2007; pp. 83–89.
14. Xiao, P.; Yu, D.C.; Yan, W. A unified three-phase transformer model for distribution load flow calculations. IEEE Trans. Power Syst. 2006, 21, 153–159. [CrossRef]
15. Choi, J.-H.; Park, D.-H. Mid-to-Long Term Operation Plan of Distribution Control Center According to Expansion of Distribution System Intelligent Equipment; Final Report; KEPCO: Naju, Korea, 2017; pp. 14–38.
16. IEEE. Standard Requirements for Instrument Transformers; IEEE: Piscataway, NJ, USA, 2016.
17. IEC. Instrument Transformers—Part 2: Additional Requirements for Current Transformers; IEC: Geneva, Switzerland, 2012.
18. Micro-PMU Data Sheet. Available online: https://www.powerstandards.com/download-center/micropmu/ (accessed on 18 February 2020).
19. IEEE. Standard for Interconnection and Interoperability of Distributed Energy Resources with Associated Electric Power Systems Interfaces; IEEE: Piscataway, NJ, USA, 2018.

Merging PMU, Operational, and Non-operational Data for Interpreting Alarms, Locating Faults and Preventing Cascades

This method uses the integration of time correlated information from Phasor Measurement Units, SCADA and non-operational data captured by other intelligent electronic devices such as protective relays and digital fault recorders, as well as their applications in alarm processing, fault location and cascading event analysis. A set of new control center visualization tools shows that the merging of PMU, operational and non-operational data could improve the effectiveness of alarm processing, accuracy of fault location and ability to detect cascades.

Introduction:

Nowadays, most of the substations are equipped with Intelligent Electronic Devices (IEDs) which can collect huge amounts of data in addition to performing their other intended functions. These IEDs include digital protective relays (DPRs), digital fault recorders (DFRs), phasor measurement units (PMUs), circuit breaker monitors (CBMs), power quality monitors (PQMs), remote terminal units (RTUs), etc[1-3]. Traditionally, RTUs constitute data acquisition part of a supervisory control and data acquisition (SCADA) system, which is the main infrastructure for monitoring and operating power system. The data continuously collected by SCADA is called "operational" data. Other types of IEDs, such as DPRs and DFRs are collecting data only when a disturbance occurs, and this data is called "non-operational" data. The "nonoperational" data collected by DPRs and DFRs plays an important role in power system alarm processing and fault analysis. PMUs are unique devices in that they collect synchronized phasors continuously, but this data has not yet been fully integrated with SCADA data. Hence, this new data is typically referred to as "situational awareness" data. In all of the above cases, collected data may be used to enhance Energy Management System (EMS) functions, and in that sense collectively the mentioned data may be called "extended SCADA" data. Integration of substation "non-operational" and "situational awareness" data with the traditional "operational" SCADA data collected by RTUs into the "extended SCADA" database to be used for new applications in the

EMS solutions is not yet explored adequately[1,4-7]. With the development of flexible electricity market operation under the deregulation rules, power system became more stressed and power network security and reliability criteria became more complex. Power systems are exposed to all kinds of disturbances. Under this situation, new tools such as intelligent alarm processor, optimized fault location and cascading event analysis[8-12], which take full use of data coming from PMUs, SCADA and other IEDs, have been proposed to help operators better analyze and control the system. Table 1 provides a summary of the data deployed in these three applications as well as their outputs expected to be presented to control center operators.

Table 1. Requirements Specification for Applications

Applications	What to Display	Data Deployed
Intelligent Alarm Processor	1. Processing of alarms; 2. Analysis result; 3. Suggested actions; 4. Additional information.	Circuit breaker control signals; SCADA measurements; Synchrophasors; Other alarm signals.
Optimized Fault Location	1. Estimated fault section (Terminal bus numbers); 2. Fault location within the estimated section; 3. Exact fault type.	IED samples of voltages and currents; Synchrophasors; SCADA measurements.
Cascading Event Analysis	1. Cascade detection; 2. Cascade classification; 3. Suggested actions.	Synchrophasors; IED samples; SCADA measurements

This method starts with the investigation of what is involved in data merging, and then continues with descriptions of the applications that use data merging. Next, the control center visualization tools which take use of data and applications are introduced. Finally the data/information exchange structure is explored. Conclusions are given at the end.

Merging of the Existing Data Sources:

The integration of PMUs, operational and non-operational data remains a challenge for several reasons. The diversity of data formats is one major problem. Non-operational data usually comes in the COMTRADE data format and IEC 61850 object model data standard for IEDs that are IEC 61850 compatible, whereas the data collected from PMUs follows the format for

synchrophasors[4-6]. In addition, data may be further formatted using the File Naming Convention Standard[7]. This makes the data merging a tedious task that requires merging of various formats before deploying them in applications. The merging of existing data sources and their applications is demonstrated in Fig. 1. While it has been proven through some recent field demonstrations by utilities and vendors that synchrophasor measurements have capability of tracking the impact of low frequency oscillations, as well as power system area frequency and angle separation, which enhances awareness of system operators, it remains an issue how user interfaces that will aid operators in making decisions should be incorporated in the existing interfaces for SCADA functions. The merging of various data sources allows implementation of a new generation of control center software aimed at automated fault location and visualization of fault disturbance consequences. The visualization tool proposed in this method seamlessly incorporates time correlated information from PMU, SCADA and non-operational data. This results in intelligent operator tools for viewing results from alarm processing, fault analysis and cascading analysis, which increases the effectiveness of power system monitoring and reduces the time needed to make decisions. The integration of data sources and the proposed control center visualization tools is shown in Fig. 2.

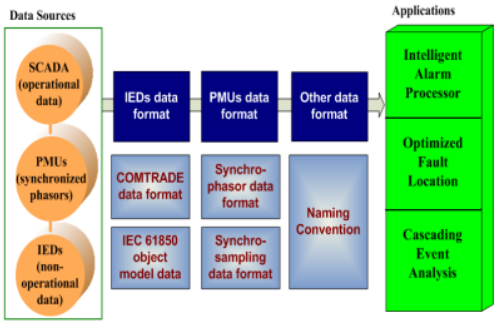

Figure 1. Data Merging and Applications

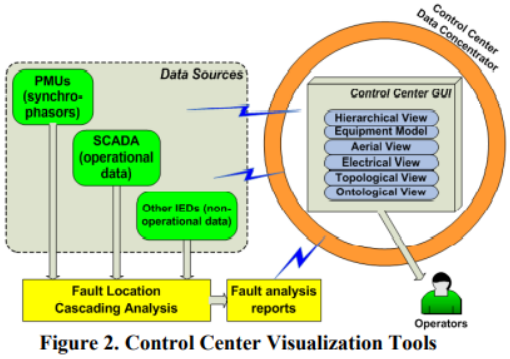

Figure 2. Control Center Visualization Tools

As shown in Fig. 2, input information such as raw samples, phasors, alarms, event files, oscillography files, etc. from PMUs, SCADA and other IEDs (e.g. DPRs and DFRs), together with automated analysis reports are collected, converted to actionable information and then sent to the control center graphical user interfaces (GUIs). After internal information processing, the graphical software will display several types of views, as outputs, using six visualization modules.

Applications Using Data Merging:

Intelligent Alarm Processor

With the growth of power system complexity, a major disturbance could trigger hundreds or even thousands of individual alarms and events, clearly beyond the ability of any control center operator to handle[8]. To adapt to the new situation, a new Intelligent Alarm Processor (IAP) has been developed to aid operators recognize the nature of the disturbances[9]. The application structure of this IAP is shown in Fig. 3. Data are collected from PMUs and other IEDs at the substation level. A wide area network (WAN) is utilized as communication link between substations and the control center. A real time database is set for storing and updating data. The different types of data are merged there. Alarms are then generated and processed at the control center engineering office. Here a Petri Net Logic algorithm is used for alarm processing. The algorithm details of this Petri Net Logic could be found in [9]. Once the alarms are prioritized and processed, the analysis results can be conveyed to the control center operators to handle the system conditions according to the recommended actions.

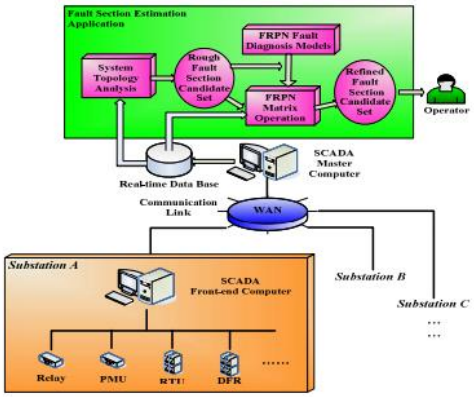

Figure 3. Intelligent Alarm Processor

Optimized Fault Location

Once a fault event in power system occurs, different IEDs automatically recognize this abnormality. It is essential that accurate information about fault location and its nature is provided as fast as possible. Various fault location algorithms have been presented in the literature in the past[10-12]. The spatial and temporal considerations indicate that there is no universal fault location algorithm suitable for all situations[1,3]. In order to be able to evaluate which algorithms are applicable for a given fault event, different data sources (measurements) have been utilized and the idea of Optimized Fault Location (OFL) approach which takes into account both temporal and spatial considerations has been proposed[10]. Fig. 4 shows an implementation of the optimized fault location. Data collected from different measurement devices are merged at the bottom layer.

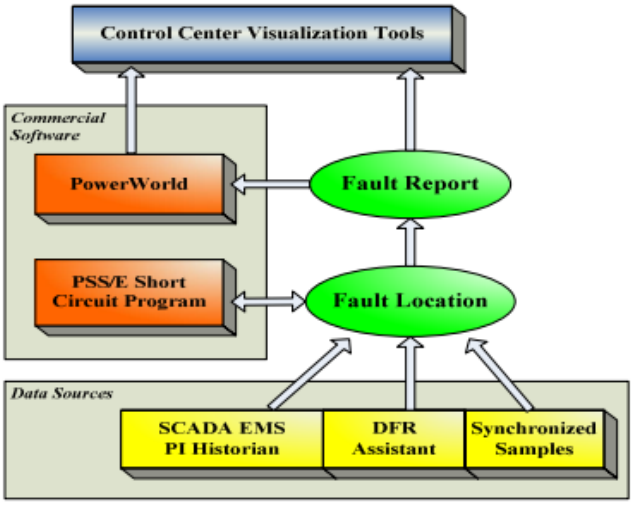

Figure 4. Optimized Fault Location

Then the selected fault location algorithm is executed, assisted by commercial data storage and viewing software, to obtain the fault location report. Once the fault location is calculated, the fault analysis report is effectively presented to operator. Knowing the real-world environment around fault location and construction of involved equipment enables utility staff to repair fault quickly and efficiently. Designing user interfaces that can effectively convey the results of fault analysis remains a challenge in the utility industry because the analysis leading to the conclusions is rather complex and operators are not trained to interpret additional information.

To overcome the above complexities that may overwhelm the operators, the user interface has to offer a compact view of the course of events with clear suggestion what the course of action should be. This is not available in today's user interface designs and requires new solution as proposed in this method.

Cascading Event Analysis

Cascading outage, especially the large-scale cascading outage, will cause great economic loss to utility companies and other businesses and potentially devastating impact on people's life. The causes for large-scale blackouts are quite unique due to the complexity of power system operations. It appears that relaying problems and inadequate understanding of unfolding events are two major contributing factors in inability to predict or prevent cascading events. Considering the above factors, a novel interactive scheme of system/local monitoring and control tools for cascading event analysis was recently introduced. The detailed techniques about how to detect, prevent and mitigate cascading events have been discussed in literature [13-16]. The local analysis tools take full use of data coming from PMU and other IEDs, including synchronized phasors and synchronized samples. Fig. 5 shows the diagrams of fault location and detection tools for the cascading analysis.

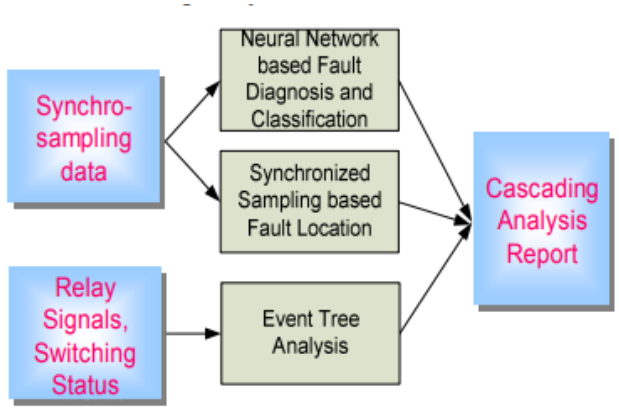

Figure 5. Cascading Event Analysis

The neural network based classifier is used to detect and classify the disturbances that require protective relay action. Comparing with traditional method, neural network based fault diagnosis algorithms usually uses the time-domain voltage and current signal samples directly as patterns instead of calculating phasors. The technique compares the input voltage and current signal

sample assembles with well-trained prototypes instead of predetermined settings. Thus accuracy of phasor measurement and relay setting coordination are not an issue in neural network based algorithms as they are in the traditional methods. This provides an advantage of the proposed solution versus the traditional methods. Voltage and current signals from the local measurement are formed as patterns by certain data processing method. Thousands of such patterns obtained from power system simulation or substation database of field recordings are used to train the neural network offline and then the pattern prototypes are used to analyze faults on-line by using the Fuzzy K-NN classifier. The use of multiple neural networks can also enhance the capability of dealing with large data set[17]. Synchronized sampling based fault location (SSFL) algorithm, as demonstrated in Fig. 6, uses raw samples of voltage and current data synchronously taken from two ends of the transmission line. Compared to the fault location algorithms that use one end or two end phasor data, synchronized sampling based fault location algorithm makes no assumptions about fault condition or system operating state, so it is immune to power swing, overload, and other non-fault situation. The sampling synchronization may be achieved by using Global Positioning Satellite (GPS) receivers, which generate the clock time reference for data acquisition equipment. This gives an accuracy and robustness advantage of the proposed scheme vs. the traditional one[12].

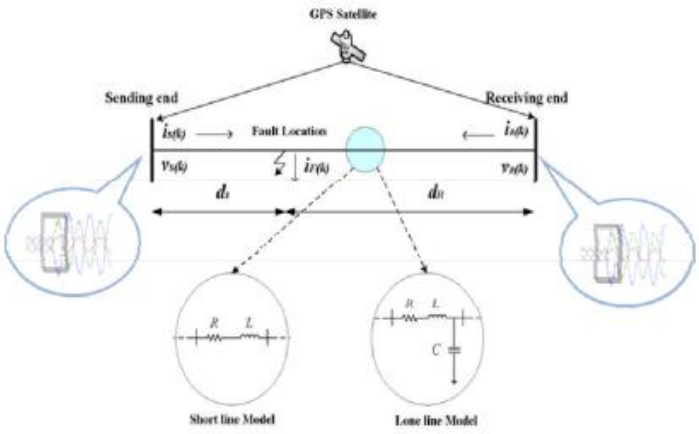

Figure 6. GPS-based SSFL

As already mentioned, compared to the fault location algorithms that use one or two end data, SSFL makes no assumptions about fault condition and system operating state. Therefore it is less affected by those factors and keeps the useful information in the waveform to locate the fault

precisely. Table 2 shows 10 cases of the results for SSFL algorithm[14]. For all the tests, the maximum error for fault classification is 3.6992%; the minimum error is 0.0234%.

Table 2. Results of SSFL algorithm

	Fault Type	Fault Distance (mile)	Fault Resistance (Ω)	Fault Angle (°)	Calculated Fault Location (mile)	Error (%)
1	CAG	85.2	3.1	199.9	85.25	0.0234
2	ABG	151.1	11.9	121.6	150.19	0.4706
3	ABCG	23.1	13.1	38.2	22.51	0.2870
4	AG	135.2	11.7	49.8	136.30	0.5693
5	CAG	116.2	1.3	217.0	115.61	0.3037
6	AB	38.3	15.1	3.8	37.48	0.3933
7	BCG	19.6	2.5	239.7	21.57	1.0016
8	CG	120.0	4.3	110.0	122.14	1.0656
9	AG	176.4	9.2	98.5	174.60	0.8917
10	ABCG	68.0	2.3	102.8	66.60	3.6992

Control Center Visualization:

This section addresses a set of new control center visualization tools, which integrate PMU, operational (SCADA) and non-operational (other IEDs) data. The proposed visualization tool also incorporates options for integration of application modules that contains state-of-the-art alarm processing, fault location and cascading analysis approaches.

System Flow Chart

The overall implementation flow chart of the visualization software is shown in Fig. 7. Embedded in the flow chart are two types of logic: external logic and internal logic. The external logic explains relationship between applications and GUI software, as well as their implementation sequence. The internal logic explains relationship and implementation sequence of various functional modules and user interfaces within the GUI software.

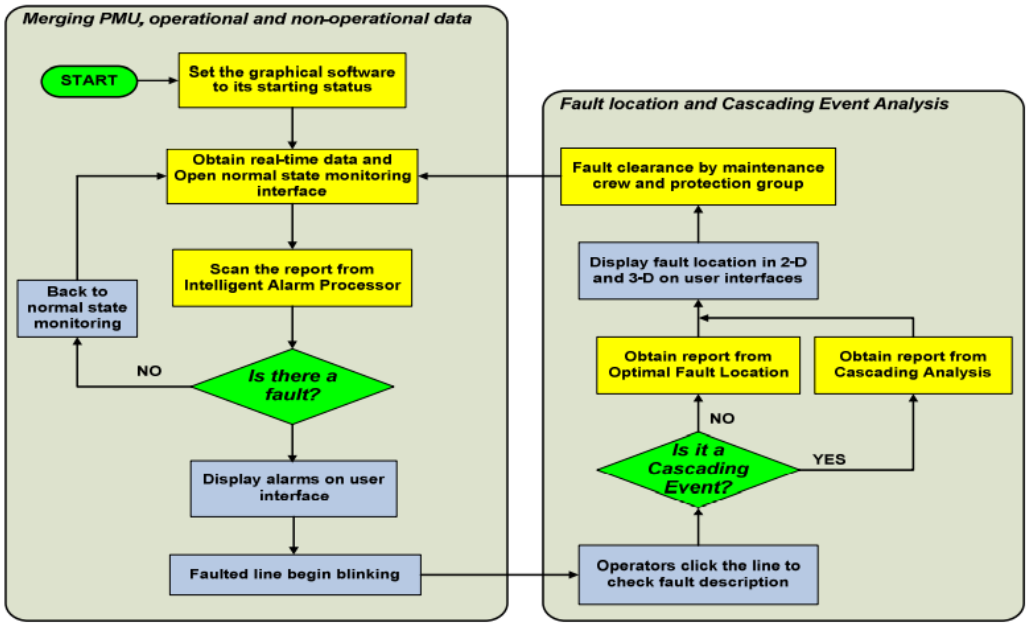

Figure 7. Visualization System Flow Chart

Visualization Tools

The proposed control center visualization system is depicted in Fig. 8. As specified in the figure, there are six modules incorporated in the proposed visualization tools: Equipment Model View, Aerial View, Electrical View, Topological View, Ontological View, and Hierarchical View

Equipment Model View:

In our proposed GUI system, various power system equipments are modeled and presented to operators through user interfaces. Currently the modeling of two types of devices has been done: Transmission Tower and Circuit Breaker.

Aerial View:

Once the fault location is calculated it is very important that the details are effectively presented to maintenance crew. The Aerial (satellite) View module translates results from fault location report files into a view of the corresponding faulted zone[18-19]. Through this module it is possible to see physical environment of the faulted area, as well as the behavior and status of equipment involved in the fault event. One example is shown in Fig. 9.

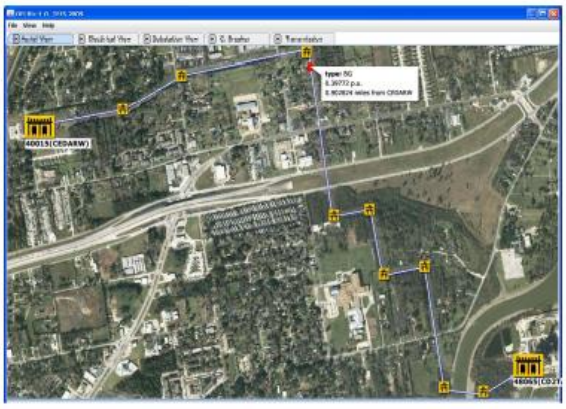

Figure 9. Aerial View

Electrical View:

This is another independent module integrated in the visualization tools. The Electrical View GUI is used to display the electrical measurements in the system on the one-line diagram, which includes the visualization of entire system connection, power flows, alarms, etc.

Topological View:

The power grid topology describes connectivity of the various components in the power system. In order to process retrieved fault event recordings, they must be related to a specific breaker/switch position from which they are measured and the information how the measurement positions were interconnected at the time of the fault occurrence needs to be known. Therefore, the system topology must be visualized.

Ontological View:

The Ontological View module relates to the application of intelligent alarm processor. The GUIs incorporated in this module display how the Petri Net Logic is executed, i.e. how the irrelevant alarms are removed and how the essential alarms are extracted. This can provide operators a comprehensive understanding of the causes and possible effects of the event.

Hierarchical View:

When system is in a normal state, real-time visualization and monitoring of the power flow and related operation are necessary. The graphical software can import real-time data by connecting to data sources that enable users to perform supervision and visual analysis of power system operations. The Hierarchical View module is used to track system behavior in normal state. Real time data are obtained from SCADA database. PI Historian was used as an example since it is widely used in the industry and because it is a time-series database designed and optimized to quickly receive, store and retrieve time-oriented data. The database could efficiently store numerical and string data, and can accommodate both small and large quantities of data for extended periods.

Control Center Work Flow Management

The control center equipped with new visualization tools will now have two distinct features comparing with those of traditional EMS system: y The substation data and extracted information are shared with different utility groups (protection engineers, dispatchers, maintenance technicians, etc.)making sure the data/information are presented in the form most suitable for a given group; y Each group receives the best information since the origin of substation data becomes transparent to the users and what they receive is the best information obtained using all available data. Each utility group will be equipped with a computer with GUI client installed. The clients together with the server are interconnected through a local area network. Operator is responsible for monitoring real-time system conditions. Other utility groups also receive information from client computers. Once an event occurs, the visualization tools will inform operator immediately. Operator could then assign tasks to different groups according to the fault reports and recommended solutions. The maintenance crew will be requested to repair system components identified with accurate fault location while protection engineers will be asked to analyze the fault clearance sequence. The dispatchers will be required to re-dispatch the power generation and load flow to balance the whole system.

Implementation of Data Merging:

When implementing the data merging, several requirements should be satisfied:

- A reliable data exchange structure should be defined;

- An effective data interpretation system should be utilized;
- Network interoperability should be maintained.

Data Exchange Structure

In order to efficiently exchange time correlated data from PMUs, SCADA and other IEDs, a data exchange system which possesses the following features is proposed:

- The Common Information Model (CIM), which is defined in IEC-61970[20], is utilized as standard data modeling format;
- After converted to CIM format, metadata is stored to an XML file. Application modules use this file to carry out analysis. Outputs from all applications are also converted to CIM format for future use;
- XML file which contains outputs of applications is sent to control center server. The server is responsible for collecting and saving data files from applications and SCADA Historian database. It is also connected to client computers through LAN. Information exchanging between server and clients is completed within the network;
- The server and client computers are connected via Java Remote Method Invocation (Java RMI). The Java RMI provides for remote communication between programs written in the Java programming language[21];
- The proposed visualization tools are installed in all client computers. Once an event occurs in power system, clients will receive fault reports from the server. Analysis results of different applications are presented to the operator through GUIs which are incorporated in the visualization tools. An entire data exchange structure between IEDs, substations, control center engineering office, utility groups, and other enterprise locations is demonstrated in Fig. 10.

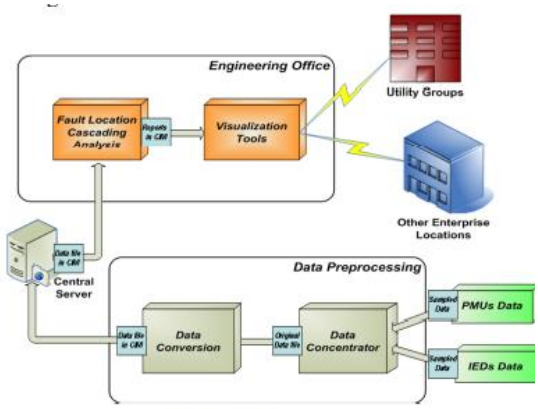

Figure 10. Data Exchange Structure

Data Interpretation

As demonstrated in Fig. 10, the PMU data, SCADA measurements and other IEDs data are collected by substation data concentrator. Since these data have different formats and contents, data preprocessing is required to convert original data and measurements into applicable data files. The data interpretation is necessary to execute this preprocessing, which is shown in Fig. 11.

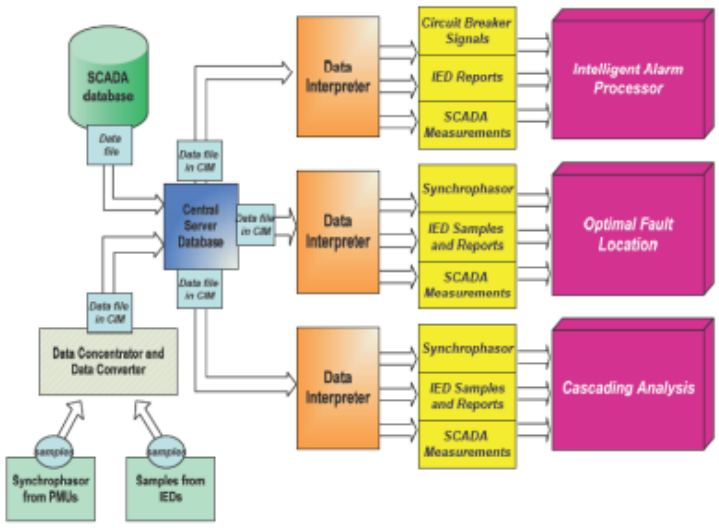

Figure 11. Data Interpretation

The data sent from control center concentrator is converted by data interpreter before they are sent to different applications. For Intelligent Alarm Processor, data is interpreted into applicable

circuit breaker signals, IED reports and SCADA measurements. For Optimized Fault Location and other applications, data is interpreted into applicable synchrophasors, IED samples and reports, as well as SCADA measurements.

Network Interoperability:

The implementation of data merging needs also to take into account the network interoperability. Several existing data communication standard are deployed to make the proposed data/application/visualization system implementation easier. As demonstrated in Fig. 12, at the substation level, IEC 61850 is deployed as the standard for intra-station data communication[5]. Ethernet is deployed for the purpose of inter-station data communication. At the control center level, IEC 61970 is the data communication standard[20].

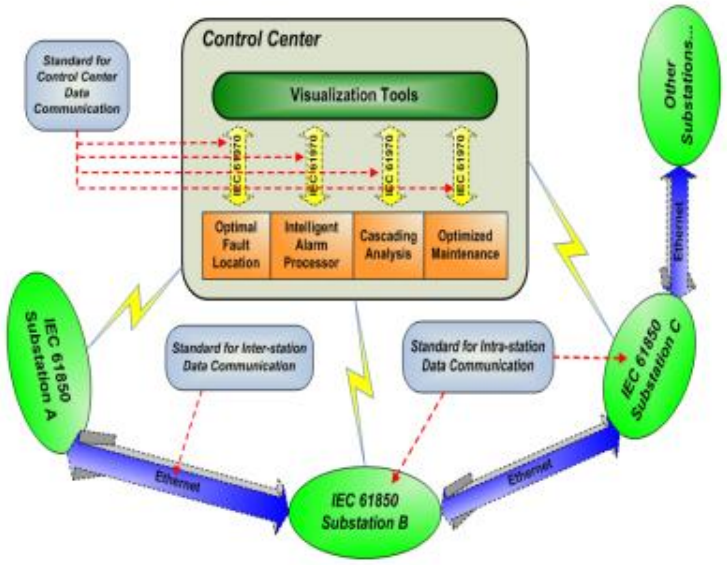

Figure 12. Network Interoperability

Conclusions:

The purpose of this research on the method is to illustrate how the efficiency of alarm processing, accuracy of fault location and capability to analyze cascades may be improved by integrating PMU, operational and non-operational data. Several accomplishments have been reported:

- The integration of time correlated information from Phasor Measurement Units, SCADA and non-operational IEDs has been implemented;
- The merging of data sources for the use in the proposed applications has been specified;
- The data processing structure as well as inputs and outputs of each application have been demonstrated and compared to the traditional implementations.
- The integrated tools for control center visualization have been designed. Six different GUI modules have been specified.
- New work flow management approach which makes better use of information extracted from the source data has been suggested.
- Implementation considerations of data merging have been discussed: data exchange structure, data interpretation, and network interoperability.

Bibliography:

1. Merging PMU, Operational, and Non-operational Data for Interpreting Alarms, Locating Faults and Preventing Cascades by Mladen Kezunovic Ce Zheng Chengzong Pang, Texas A&M University.
2. M. Kezunovic, M. Knezev, "Temporal and Spatial Requirements for Optimized Fault Location," 41th Annual Hawaii International Conference on System Sciences, Waikoloa Village, Big Island, Hawaii, January 2008.
3. PSerc Project S-25 Final Report (08-12), “Effective power system control center visualization”. [Online] Available: http://www.pserc.org
4. M. Kezunovic, A. Abur, "Merging the temporal and spatial aspects of data and information for improved power system monitoring applications," IEEE Proceedings, Vol. 9, Issue 11, pp 1909-1919, 2005.
5. IEEE Standard Common Format for Transient Data Exchange (COMTRADE) for Power Systems, IEEE Std. C37.111-1999 (Revision of IEEE Std. C37.111-1991).
6. IEC 61850 – Communication networks and Systems in Substations, IEC Standard, 14 parts, 2002 -2004.
7. IEEE Standard for Synchrophasors for Power Systems, IEEE Std. C37.118-2005 (Revision of IEEE Std. 1344-1995).
8. M. Kezunovic, et al, "IEEE Recommended Practice for Naming Time Sequence Data Files," IEEE Std. C37.232- 2007.
9. W. Prince, B. Wollenberg and D. Bertagnolli, "Survey on excessive alarms," IEEE Transactions on Power Systems, Volume 4, Issue 3, pp. 188-194, August 1989.
10. X. Luo, M. Kezunovic, "Implementing Fuzzy Reasoning Petri-nets for Fault Section Estimation," IEEE Transactions on Power Delivery, Vol. 23, No. 2, pp. 676-685, April 2008.
11. PSerc Project T-32 Final Report (08-07), “Optimized Fault Location”. [Online] Available: http://www.pserc.org
12. C.S. Chen, C.W. Liu, J.A. Jiang, "A New Adaptive PMU-Based Protection Scheme for Transposed/Untransposed Parallel Transmission Lines," IEEE Transactions on Power Delivery, Vol. 17, Issue 2, pp. 395-404, April 2002 [12] M. Kezunovic, B. Perunicic, "Automated transmission line fault analysis using synchronized sampling at two ends," IEEE Transactions on Power Systems, Vol. 11, No. 1, February 1996.
13. PSerc Projcet S-19 Final Report (05-59) - Part I, "Detection, Prevention and Mitigation of Cascading Events". [Online] Available: http://www.pserc.org

14. PSerc Project S-29 Final Report (08-18) - Part I, "Detection, Prevention and Mitigation of Cascading Events". [Online] Available: http://www.pserc.org
15. H. Song, and M. Kezunovic, "A New Analysis Method for Early Detection and Prevention of Cascading Events," Electric Power Systems Research, Vol. 77, Issue 8, Pages 1132-1142, June 2007
16. C. Pang, and M. Kezunovic, "Information Management System for Detecting Cascading Events," PowerCon 2008 & 2008 IEEE Power India Conference, New Delhi, India, Oct. 2008.
17. S. Vasilic, M. Kezunovic, "Fuzzy ART Neural Network Algorithm for Classifying the Power System Faults," IEEE Transactions on Power Delivery, Vol. 20, No. 2, pp 1306- 1314, April 2005.
18. S. Kocaman, L. Zhang, A. Gruen, D. Poli, "3D City Modeling from High-resolution Satellite Images," ISPRS Ankara Workshop 2006, Ankara, Turkey, Feb. 2006.
19. Yoshihiro Kobayashi, George Karady, et al, "Satellite Imagery for the Identification of Interference with Overhead Power Lines," Project Final Report, PSERC, Jan. 2008.
20. IEC 61970: Energy Management System Application Program Interface (EMS-API) – Part 301: Common Information Model (CIM) Base, Revision [6].
21. William Grosso, "Java RMI," Sebastopol, CA: O'Reilly Media, 2002.

5. CONCLUSION:

These were several different methods and techniques for fault location in distribution networks using PMU which offer a comprehensive analytical study for the unique types of PMUs and synchrophasor systems being developed allowing assessment of the system-wide impact of synchrophasor measurement errors during faults. There were a lot of varying approaches and all of them shows us that using PMU we can recognize faults and address them at a significantly lower amount of time which in turn increases the efficiency. There are several other studies and researches which in this world of revolution are being worked on every single day. In this age of advancement I believe that PMUs are the future to look towards improving the distribution network.

Acknowledgements:

In the name of Almighty Allah, the most gracious and merciful, who gave me the ability, self-belief and mental fortitude to complete this thesis. My foremost expression of submission and gratitude goes to Almighty Allah without whose grace and mercy; this work would never have been possible even in the slightest.

I would like to express my sincere gratitude to my supervisor, Professor Lorenzo Peretto for giving me the opportunity and believing in me to do my master's thesis under him. His trust and direction, as well as his encouragement and support, especially during extremely difficult moments, has helped me to never lose hope and give my absolute best while completing this thesis. I will forever be grateful to him because of this and will always encourage other students having interest in the same area to pursue their thesis under his supervision.

I can never imagine the words which could perfectly and completely describe my gratitude to my parents for their unwavering support, love, prayers, and best wishes for my success. Their efforts, sacrifices and encouragements are the reason I was able to pursue higher education to this level and helped me become the person I am today. I also want to express my gratitude to my younger brothers who always have treated me with love as well as respect and encouraged me to be better and it is because of them that I always want to be a good example for others as well as them to follow. I'd also like to extend my gratitude to my fiancée for her unwavering faith and support in every step of my life.

Finally, I would like to thank my friends for their encouragement, fun times and their presence which helped me deal with a lot of dark and trying times.